SUPPLEMENTAL MATERIAL

Bioengineering Human Myocardium on Native Extracellular Matrix

JP Guyette[1,2], JM Charest[1], RW Mills[3], BJ Jank[1,2], PT Moser[1,2], SE Gilpin[1,2], JR Gershlak[4], T Okamoto[1], G Gonzalez[1,2], D Milan[3,5], GR Gaudette[4], HC Ott[1,2,6,7]

METHODS

Human Heart Preparation and Decellularization. In collaboration with the New England Organ Bank (NEOB), donated human hearts that were not suitable for transplantation were retrieved for research after consent (n = 67; 5 patient records unavailable). Documented records from recovered hearts indicate there were 32 male donors, 30 female donors, an average age of 53 ± 14 years, and an average body mass index of 27.78 ± 6.25. Human hearts were recovered in standard fashion and delivered to Massachusetts General Hospital, with an average cold ischemia time of 455 ± 184 minutes. All human tissue experiments were performed in accordance with institutional guidelines and approved by the Partners Human Tissues Research Committee at the MGH. Informed research consent was required by all human donors, which was obtained by the NEOB. Hearts were randomly assigned to experimental groups as they were received; 38 hearts were designated for pressure- controlled perfusion decellularization and 29 hearts were maintained to satisfy the control group. Twenty-four hearts were retrieved from donation after cardiac death (DCD) donors, and the remaining hearts were recovered from donation after brain death (non-DCD) donors. Upon delivery, the custom decellularization chamber was assembled and the aorta was cannulated in a biological safety cabinet, using sterile gloves and aseptic technique. The heart was placed in a sterilized organ decellularization chamber, and the aortic cannula connected to an in-chamber perfusion line of the pressure-controlled pump system.[1] Anterograde coronary perfusion was applied for a constant pressure of 60 mmHg at room temperature, using a feedback control unit to regulate and record pressure and flow. Hearts were aseptically decellularized with the following succession of solutions: phosphate buffered saline with 1 U/mL heparin (1 hour); 1% sodium dodecyl sulfate (SDS) in deionized water (168 hours); deionized water (DI H2O, 24 hours); 1% Triton-X in deionized water (24 hours); phosphate buffered saline (168 hours). Decellularization was visually confirmed by an opaque appearance of the cardiac ECM, accompanied with a loss of tissue turgor and rigidity (**Fig. 1A**). Analysis of recorded data indicated trends towards increased coronary flow and subsequent decreased vascular resistance over the course of the decellularization process (**Fig 2A,B**), but differences were not statistically significant. In addition, a comparison of decellularizing DCD and non-DCD hearts showed that DCD hearts appeared to have lower coronary flow and higher vascular resistance, however, differences were not statistically significant (**Fig. 2A,B**). Following decellularization, hearts were decannulated and stored in PBS with antibiotics/antimycotics at 4°C.

SDS, DNA, GAG, Collagen, and Elastin Quantification**.** Biochemical analysis of human heart samples (cadaveric and decellularized) was performed to determine the presence of extracellular matrix proteins (insoluble collagen, soluble collagen, elastin, and glycosaminoglycans) and DNA. Hydroxyproline content as a measure of insoluble collagen was quantified using the Hydroxyproline Assay Kit, as per the manufacturer's instructions (Sigma-Aldrich, St. Louis, MO). Soluble collagen, alpha-elastin, and sulfated glycosaminoglycans were quantified using the Sircol, Fastin, and Blyscan assay kits, respectively (Biocolor, UK). For DNA quantification, tissue samples were digested overnight at 55 °C in 310 µL of a solution containing 10 mM Tris (pH = 8.0), 5 mM EDTA, 0.1 M NaCl, 1% SDS, and 650 µg/mL Proteinase-K (Life Technologies, Carlsbad, CA). Double-stranded DNA (dsDNA) was then isolated using a phenol/chloroform extraction and alcohol precipitation, and quantified using the Quant-iT PicoGreen dsDNA kit (Life Technologies). All biochemical data is presented as the total mass of the component extracted normalized to tissue sample wet weight in Figure 1, and normalized to dry weight (lyophilized tissue) in Supplemental Figure II[2]. The mean dry weight of all tissue samples was 2.7 mg. For each component (except DNA), biochemical analysis was carried out for three locations (anterior free wall, septum, and apex) on each heart. An analysis of variance revealed no difference in component content between locations. Thus, for each component the values for the three locations on a given heart were averaged to obtain a representative value for that heart. DNA values were obtained from one septum tissue sample per heart. For endonuclease treatment of acellular cardiac matrices, biopsies were taken before and after whole-organ perfusion with 1 L of Pierce Universal Nuclease (25 U/mL) for 24 hours. All samples were processed and analyzed for dsDNA quantification using the Quant-iT PicoGreen dsDNA kit, as described above.

LC-MS/MS Proteomic Matrix Analysis. Both cadaveric and decellularized heart tissue samples were first homogenized and sonicated in radioimmunoprecipitation assay (RIPA) buffer, and spun down to collect supernatant. A chloroform/methanol/water protein precipitation was performed, and washed twice. The protein pellet was solubilized in Rapigest, treated with DTT/IAN, and digested with Lys-C/Trypsin. Samples were quantified using a Nanodrop and run on a microcapillary tandem mass spectrometry (LC-MS/MS) Q-Exactive Plus system, with long gradient for label-free quantification. Acquired proteomics data was processed using Progenesis QI software. Two distinct areas of the left ventricle in 3 different hearts were analyzed for each group, for a total of 12 samples (6 cadaveric myocardium, 6 decellularized myocardium). The subcellular location of each identified human protein was then determined using the Universal Protein Knowledge Base (UniProtKB, www.uniprot.org, accessed on Feb. 21st, 2015).[3] All identified proteins (proteome) whose subcellular location included either the extracellular matrix or basement membrane were designated as part of the matrisome.[4]

Biaxial Mechanical Testing of Myocardium. Two-dimensional (2D) tensile testing was performed on cadaveric and decellularized heart samples. Full-thickness samples of approximately 25 x 25 mm were cut from the anterior wall of the left ventricle. Sample width, length, and thickness were measured using a micrometer. Four graphite dots were glued to the surface of each specimen for tracking displacement. Two sutures (2-0 silk) were placed approximately 2 mm from the edge in each side of the sample and tied creating a loop approximately 5 cm in length. The sutures were looped around pulleys on a custom planar biaxial test device. Room temperature PBS was used to float the samples in the testing chamber and the tare load was set when the sutures were under tension and the load increased slightly (~0.2 kPa). Loads were applied bi-axially (1:1 ratio of x-load to y-load) under stress control up to 20 kPa. The forces along the axes were measured with torque transducers and the movement of the graphite particles was measured using a CCD camera. The stress was calculated as the force acting on the cross-sectional area and the strain was calculated as the change in length divided by the original length at the tare load. For each sample, moduli were calculated as the slope of the linear region of the stress-strain curve. To quantify the degree of anisotropic behavior exhibited by the moduli of the tissue samples, an anisotropy ratio was calculated for each tissue sample; where, anisotropy ratio = $|Ex – Ey| / (Ex + Ey)$. Thus a ratio close to zero would indicate little or no anisotropy and a ratio close to one would indicate a high degree of anisotropy.

Immunogenic Profiling of Decellularized Human Cardiac Scaffolds. **Overview:** Twelve rats were randomly divided into 4 equal groups of 3 each. Cardiac material was implanted subcutaneously in 3 experimental groups, while the sham operated group underwent the procedure for the subcutaneous pocket but did not receive an implant. The cardiac materials implanted were decellularized human heart, cadaveric human heart, or decellularized porcine heart. All animals were sacrificed at 2 weeks after implantation. At the time of sacrifice, blood samples were taken from each rat for whole blood and serum analysis. In addition, the explanted tissues were examined using immunohistochemical methods for cell surface markers representative macrophage profiles (i.e. M1, M2). All procedures were performed in accordance with the National Institutes of Health guidelines for care and use of laboratory animals, and with approval of the Institutional Animal Care and Use Committee at the Massachusetts General Hospital. **Animals and Surgical Procedure:** Male, Sprague-Dawley rats weighing 300 to 500 g were purchased from Charles River Laboratory (Wilmington, MA). Each animal was maintained on a diet of dry food and housed individually in an environment maintained at 68-76° C for 24 h a day, with a light/dark cycle of 12/12 hours. During the surgical procedure, a 1.0 cm^2 subcutaneous pocket was created along the sagittal plane of the dorsal surface of each animal (between the two scapulae), as previously described.[5, 6] All animals were survived for 2 weeks, at which point they were sacrificed by exsanguination during blood collection analysis. **Cardiac Material:** Three types of cardiac material were prepared: cadaveric human myocardium, decellularized human cardiac matrix, and decellularized porcine cardiac matrix. Pieces of cardiac material from fresh cadaveric myocardium or freshly decellularized cardiac matrix were cut to 0.5 cm^3 volumes. Cadaveric and decellularized human cardiac material was obtained through our collaboration with the New England Organ Bank, as described above. Decellularized human cardiac matrix was prepared as described above. Cadaveric and decellularized rat cardiac material was harvested from Sprague-Dawley rats weighing 300 to 500 g were purchased from Charles River Laboratory (Wilmington, MA). Decellularized porcine cardiac matrix was prepared as previously described.[1] **Whole Blood Analysis:** Whole blood was collected from each rat in Vacutainer® tubes (BD Biosciences, Franklin Lakes, NJ), spun down as per manufacturer recommendation, and stored at 4°C until analysis. Samples were run on a HESKA HemaTrue Analyzer (HESKA, Loveland, Colorado), and values from rats in each group were averaged for each component. **Immunohistological Analysis:** Implanted materials were harvested with an equal amount of adjacent fascia tissue. The specimens were fixed in 10% neutral buffered formalin and embedded in paraffin. Serial sections of the embedded tissue specimens were then cut at 5 µm. The tissue sections were stained with hematoxylin and eosin, and representative sections were prepared for immunohistochemical staining by deparaffinization with xylene and rehydration through a graded ethanol series. A heat-mediated antigen retrieval technique that included a 20-min boil in 0.01 M citrate buffer, pH 7.0 was used. Once cooled, 3 separate washes of phosphate buffered saline (PBS) were applied (5 min each). Primary antibody dilutions were made with blocking buffer and were as follows: mouse anti-rat CD68 (cat#: MCA341GA; AbD Serotec, Raleigh, NC) at 1:50 dilution in PBS, rabbit anti-CD80 (cat#: bs-2211R; Bioss, Inc., Woburn, MA) at 1:100 dilution, and rabbit anti-rat CD163 (cat#: bs-2527R; Bioss, Inc.) at 1:100 dilution. Secondary antibodies were applied for 1 hour at room temperature (25°C). Secondary antibody dilutions were made with blocking buffer, as follows: 1:400 anti-mouse 488 and 1:400 anti-rabbit 594 (both from Invitrogen, Eugene, OR). A CellProfiler image analysis pipeline was used to quantify macrophage phenotype across images (Supplemental Fig. V).[7] **HLA Analysis:** Sera was collected from each rat in Vacutainer® tubes (BD and Company, Franklin Lakes, NJ), spun down as per manufacturer recommendation, and stored at 4°C until analysis. Sera was run against Panel Reactive Antibody (PRA) single-antigen beads, using clinical test kits for LABScreen PRA Class I and II (cat#'s: LS1PRAS and LS2PRAS; One Lambda, of Thermo Fisher Scientific, Canoga Park, CA). The secondary antibody used to detect antigen-reactive rat antibodies was R-Phycoerythrin[1]-conjugated AffiniPure, goat anit-rat IgG (cat #: 112-116-071; Jackson ImmunoResearch Laboratories, Inc, West Grove, PA). Samples were run through a Luminex IgG-assay, using a LABScan100™ Luminex analyzer, equipped with xPONENT software (Life Technologies, Grand Island, NY). The LABScan100™ Luminex required a 100-event minimum per sample to determine a successful test read-out. Using HLA Fusion Software (version 3.0; One Lambda, of Thermo Fisher Scientific, Canoga Park, CA) for post-processing, experimental samples were analyzed using the sham group as a reference, and histograms we generated by the software by plotting mean fluorescence intensity (MFI) attributed to beads with specific HLA alleles (**Fig. 1Ki,ii**). **HLA Immunohistochemistry:** Freshly prepared samples were fixed in 10% neutral buffered formalin, embedded in paraffin, and sectioned at 5 µm. Sections were deparaffinized with xylene and rehydration through a graded ethanol series, and then treated for 30 minutes in citrate buffer at 95°C for antigen retrieval. Primary antibodies were allowed to attach overnight at 4 °C. Primary antibody dilution was made with blocking buffer as follows: 1:100 anti-HLA 1 ABC [EMR8-5] (cat#: ab70328;

Abcam, Cambridge, MA). Secondary antibody was applied for 1 hour at room temperature (25°C). Secondary antibody dilution was made with blocking buffer, as follows: 1:400 anti-mouse 594 (Invitrogen, Eugene, OR). Images were recorded using a Nikon Eclipse TE200 microscope (Nikon, Melville, NY).

***Histology and Immunocytochemistry*.** For immunohistochemistry, tissue samples were fixed in 5% formalin, paraffin-embedded, and sectioned following standard protocols. Briefly, 5 µm sections were deparaffinized, and treated for 30 minutes in citrate buffer at 95°C for antigen retrieval. Primary antibodies were allowed to attach overnight at 4 °C. Primary antibody dilutions were made with blocking buffer, as follows: 1:50 anti-laminin G1 (cat#: sc-13144; Santa Cruz Biotechnology, Dallas, TX), 1:50 anti-elastin (cat#: sc-58756; Santa Cruz Biotechnology), 1:50 anti-fibronectin (cat#: sc-59826; Santa Cruz Biotechnology), 1:100 anti-collagen I (cat#: ab6308; Abcam, Cambridge, MA), 1:300 anti-collagen III (cat#: ab6310; Abcam), 1:200 anti-MHC (cat#: ab15, anti-heavy chain cardiac myosin antibody [3-48]; Abcam), 1:50 anti-collagen IV (cat#: LS-C79592; Lifespan Biosciences, Seattle, WA). Anti-mouse conjugated to HRP was added at 1:100 for 30 min, and subsequently developed with 3,3'-diaminobenzidine (Dako, Carpenteria, CA) until good staining intensity was observed. Images were recorded using a Nikon Eclipse TE200 microscope (Nikon, Melville, NY).

For cardiac fiber preparations, recellularized fibers were first washed with PBS and then fixed with 5% formalin for 24 hours at 4°C prior to paraffin embedding. For whole-heart preparations, recellularized scaffolds were perfusion-fixed with recirculating 5% formalin through the left main coronary artery, at 20 mL/min for 3 hours at 25°C. Scaffolds were then systematically processed by excising the reseeded region from the matrix. Reseeded regions were cut into defined tissue blocks from base to apex (for samples with 0.5 cm thickness), and then tissue blocks were placed in cassettes and submerged in 5% formalin for 24 hours.

Tissue samples for both reseeded fibers and reseeded hearts were paraffin-embedded, sectioned, and stained following standard protocols. Briefly, 5 µm sections were deparaffinized, and treated for 30 minutes in citrate buffer at 95°C for antigen retrieval. Primary antibodies were allowed to attach overnight at 4 °C. Primary antibody dilutions were made with blocking buffer and were as follows: 1:100 anti-sarcomeric α-Actinin (cat #: A8711, Sigma-Aldrich, St. Louis, MO), 1:100 anti-myosin heavy chain (cat #: SC-20641, Santa Cruz Biotechnology, Dallas, TX), and 1:100 anti-troponin T (cat #: ab8295, Abcam Inc., Cambridge, MA). Secondary antibodies were applied for 1 hour at room temperature (25°C). Secondary antibody dilutions were made with blocking buffer, as follows: 1:400 anti-mouse 488, 1:400 anti-mouse 594, 1:400 anti-rabbit 594 (all from Invitrogen, Eugene, OR). TUNEL assay was performed using the DeadEnd™ Fluorometric TUNEL System per the manufacture's protocol (Promega Corporation, Madison, WI). Tissues slides were mounted with Dapi Fluoromount-G (Southern Biotech, Birmingham, AL). Masson's Trichrome was performed using reagents and methods based on kit manufacturer's recommendations (American MasterTech, Lodi, CA). Images were recorded using a Nikon Eclipse TE200 microscope (Nikon, Melville, NY).

In a systematic histological analysis of whole-heart experiments, reseeded regions were cut into defined tissue blocks as described above. Tissue sections from each tissue block were then immuno-stained for myosin heavy chain (MHC) for immunofluorescence detection, as described in the previous paragraph. By measuring the areas of MHC-positive signal in several tissue sections throughout the reseeded regions (from base to apex), we applied linear interpolation along with respect to the vertical dimension to estimate a volumetric recellularization.

***Vascular Histology*.** Samples of the left anterior descending (LAD) coronary artery were cut to 5 µm cross-sections, which were then deparaffinized through xylene and alcohol washes. Pentachrome staining was performed using the Russel-Movat Pentachrome Stain Kit Procedure, as per manufacturer's instructions (American MasterTech, Lodi, CA).

Scanning Electron Microscopy of LAD. A cross sectional biopsy of a cadaveric and decellularized left anterior descending arteries were fixed in half-strength Karnovsky's fixative after harvest, and stored for 24 hrs at 4°C. They were then rinsed in PBS, dehydrated through graded ethanols, critical point dried (Autosamdri 795 Supercritical Point Dryer; Tousimis, Rockville, MD), mounted on specimen holders, and sputter coated with Chromium in an ion beam coater (model 681; Gatan, Pleasanton, CA). Images were acquired via a field emission scanning electron microscope (JSM-7401F; JEOL Ltd., Peabody, MA).

Coronary Angiography. All hearts were mounted with a cannula in the ascending aorta. Antegrade flow was created via pumping normal saline through the cannula at a constant pressure into the aortic root. Coronary angiography was then performed by selectively engaging each of the coronary artery with the 5F Judkins catheters. Coronary cine was obtained using a GE OEC 9600 c-arm with injections of Visipaque (1mL contains 652 mg of iodixanol which is 320 mg organically bound iodine) contrast. Cines and still frame images were then captured onto USB via MediCapture.

Microfil® Preparation, µCT, and Analysis of Coronary Microvasculature. **Microfil® Preparation:** Tissue samples were prepared by first accessing and cannulating the left and right main coronary arteries in the whole-heart sample (either a cadaveric human heart or an intact acellular human cardiac scaffold). Hearts were perfused with sterile PBS at a constant infusion pressure of 60 mm Hg for 15 minutes to recruit vasculature and to visualize constant flow from the coronary sinus. Once the matrix was rehydrated and vascular conduits were recruited, radiopaque Microfil® silicon-based injection compound (MV-122, Flowtech, Carver, MA) was perfused into the matrix at a constant pressure of 60 mm Hg. Microfil® perfusion was stopped when injection compound was observed flowing from the coronary sinus. At this time, perfusion tubing was clamped off and the Microfil®-infused heart was allowed to sit for 90 minutes at room temperature for the compound to cure. Hearts were then placed in 70% ethanol, and allowed to cure further at 4°C for 24 hours. **µComputed Tomography (µCT):** Once fully cured, full-thickness samples were excised identifying a region of the LAD mid-way between the apex and base of the heart, and then cutting a tissue cube with a 1x1 cm^2 surface area that spanned from the epicardium to the endocardium. Tissue cubes were stored in 70% ethanol until being scanned. µCT imaging was performed on a piece of human heart using a high-resolution desktop imaging system (µCT40, Scanco Medical AG, Bruttisellen, Switzerland). Transverse slices were acquired with 6 μm^3 isotropic voxel size, 70 kVp peak x-ray tube potential, 114 uA intensity, 300 ms integration time, and were subjected to Gaussian filtration. The resulting images were segmented based on voxel intensity in order to select the vascular regions and 3D reconstructions were generated. **Post-µCT Analysis of µVasculature:** Two-dimensional µCT images were analyzed for distribution and diameter. Image stacks from full-thickness samples were first assessed to determine the starting epicardial slice and the ending endocardial slice, and then the number of images was divided into equal thirds to determine epicardial, mid-myocardial, and endocardial sub-regions. At least 3 representative images in each sub-region were analyzed, separated by 600-1200 µm, so as to assess the vascular landscape through the sub-regional thickness. Vessel densities were determined for each 2D image and normalized to the analyzed tissue area, and images within sub-regions were averaged. Using ImageJ to measure the minor axis of vessel cross-sections, each 2D image was analyzed and binned for vessel diameters in each sub-region. **µOptical Coherence Tomography (µOCT) of Perfused µVasculature:** To visualize perfusion through microvasculature in decellularized human hearts, large full-thickness sections of myocardium were first excised along the left anterior descending coronary artery. Epicardial conductance arteries were then cannulated, perfused with sterile phosphate buffered saline (PBS), and major peripheral leaks were shunted with microvascular clips.

A 50 mL mixture of red fluorescent microbeads (2.06 µm diameter; cat #: FH-2040-2, Spherotech, Lake Forest, IL) was then prepared to a dilution of 1:100. Diluted microbeads were then gravity-perfused through the full-thickness piece of decellularized myocardium at 30 mm Hg. During gravity-perfusion of microbeads, micro-optical coherence tomography (µOCT) was used to acquire image stacks ~200 µm below the surface of the cut mid- and endocardium, at a frame rate of 40 fps for 30 seconds (µOCT method described below). Image analysis was completed using ImageJ software, equipped with a Running Z Projector plugin, set to a running average size of 20, for maximum intensity projection.

Cell Culture, Cardiac Differentiation of iPS Cells, and Cell Characterization. **iPS Culture:** Human cardiomyocytes were generated from the BJ-RiPS-1.1 cell line obtained from the Harvard Stem Cell Institute, sourced from human BJ postnatal fibroblasts transfected with mRNAs encoding Klf4, c-Myc, Oct4, Sox2, and Lin28[8]. Passage 18-30 undifferentiated BJ-RiPS were cultured on growth factor reduced Matrigel™ (diluted 1/100; cat. # CB 40230, Thermo Fisher Scientific Inc, Waltham, MA), in mTeSR™1 media (cat. # 05870, Stem Cell Technologies Inc, Vancouver, BC, Canada). **Cardiac Differentiation:** Cardiac differentiation of BJ-RiPS cells was performed using an established protocol based on a temporal modulation of Wnt signaling with small molecules (Stemolecule™ CHIR99021, cat. # 04-0004-02; Stemolecule™ Wnt Inhibitor IWP-4, cat. # 04-0036; Stemgent Inc, Cambridge, MA) [9]. Cardiomyocyte generation was confirmed by observation of functional contractility of beating cells *in vitro*. Cardiomyocytes were maintained in RPMI 1640 medium (cat. # 11875-119, Life Technologies, Grand Island, NY) supplemented with B-27 (cat. # 17504-044, Life Technologies), with media changes every 2 days. Human iPS-derived cardiomyocytes were cultured for at least 20 days after the onset of differentiation before being harvested for recellularization experiments. **Cell Characterization – RT-PCR:** Over the time-course of differentiation (days 0, 3, 5, 7, 14, 30, 60, 120, and 180), differentiating iPS cells were scrapped off of culture plates, pelleted down by centrifugation (300 g, 5 min), and stored in RNAlater (cat#: AM7020; Life Technologies, Grand Island, NY) at 4°C until analyzed. RNA was extracted using an RNeasy® Plus Mini Kit (cat#: 74134; Qiagen, Valencia, CA), and quantified using a NanoDrop 2000 Spectrophotometer (Thermo Scientific, Waltham, MA). cDNA was prepared using a SuperScript® III First-Strand Synthesis SuperMix Kit for qRT-PCR (cat #: 11752-050; Life Technologies, Grand Island, NY). Quantitative RT-PCR was performed using TaqMan® Gene Expression Master Mix (cat. #: 4369016; Applied Biosystems, Foster City, CA), along with the following TaqMan® Probes (all from Applied Biosystems): Oct4 (cat #: HS00999632_g1), Sox2 (cat #:HS04407947_m1), Nanog (cat #: HS04260366_g1), MIXL1 (cat #: HS00430824_g1), T (cat #: HS00610080_m1), ISL-1 (cat #: HS0015126_m1), TBX2 (cat #: HS00911929_m1), GATA4 (cat #: HS00171403_m1), Nkx2.5 (cat #: HS00231763_m1), MEF2C (cat #: HS00231149_m1), TBX5 (cat #: HS00361155_m1), MYH6 (cat #: HS01101425_m1), MYH7 (cat #: HS0110632_m1), MYL2 (cat #: HS00166405_m1), TNNT2 (cat#: Hs00943911_m1), and 18S (cat #: HS99999901_s1). Samples were run on a StepOnePlus Real-Time PCR System (Applied Biosystems), and analyzed using the delta-delta CT method with respect to sample's internal 18S signal and fold-differences to undifferentiated iPS cells. **Cell Characterization – Immunocytochemistry:** BJ RiPS-derived cardiomyocytes between days 30 and 60 post-differentiation were washed once with PBS, and then fixed with 4% paraformaldehyde for 15 minutes at 4°C. Cells were then washed three times with PBS, and then permeabilized with 1.5% Triton-X solution for 10 minutes. Cells were then washed three times with PBS, and then blocked with 1.5% donkey serum for 30 minutes. Following blocking, primary antibodies were allowed to attach overnight at 4 °C. Primary antibody dilutions were made with blocking buffer and were as follows: 1:100 anti-sarcomeric α-Actinin (cat #: A8711, Sigma-Aldrich, St. Louis, MO), 1:100 anti-myosin heavy chain (cat #: SC-20641, Santa Cruz Biotechnology, Dallas, TX), and 1:100 anti-troponin T (cat #: ab8295, Abcam Inc., Cambridge, MA). Secondary antibodies were applied for 1 hour at room temperature (25°C). Secondary antibody dilutions were made with blocking buffer, as follows: 1:400 anti-mouse 488, 1:400 anti-mouse 594, 1:400 anti-rabbit 594 (all from Invitrogen, Eugene, OR). Cell nuclei were stained with Hoechst dye (cat. #: H3570, Thermo Fisher Scientific, Inc., Waltham, MA), washed three times with PBS, and imaged in PBS. For some cell preparations, cytoskeletal actin structures were counterstained with Phalloidin stain (cat. #: O7466, Thermo Fisher Scientific, Inc.) for 20 minutes between the blocking step and application of primary antibody. **Cell Characterization – Flow Cytometry:** iPS-derived cardiomyocytes between days 30 and 60 post-differentiation were washed twice in phosphate buffer saline (PBS) and dissociated into single cells by treatment with 0.05% trypsin/EDTA. For the detection of cardiac sarcomeric α-actinin and cardiac troponin T independently, the cells were fixed with 4% paraformaldehyde at room temperature for

20 min, followed by 2 PBS washes. Cells were then permeabilized with 0.1% Triton X-100 in PBS on ice for 20 min, washed twice with PBS, and centrifuged at 300 g for 5 min. Cells were blocked with 1% BSA in PBS for 30 min, and then incubated with the primary antibody at room temperature for 1 h. After washing in PBS, the cells were incubated with the secondary antibody at room temperature for 1 h. After washing in PBS, the cells were suspended in 400 µl PBS and assayed by flow cytometry (FACS Calibur; BD Biosciences, Franklin Lakes, NJ). Mouse IgG anti-α-sarcomeric-actinin (cat #: A7811, 1:100; Sigma, St. Louis, MO) and mouse IgG cardiac troponin T (cat #: ab8295 – [1C11], 1:100; Abcam, Cambridge, MA) served as primary antibodies. The secondary antibody was goat anti-mouse 488 (cat#: A-11001, 1:400; Invitrogen, Eugene, OR). Cells stained with primary isotype control antibody (normal mouse IgG_1; cat. #: sc-3877, Santa Cruz Biotechnology, Dallas, TX) and secondary fluorescence-conjugated antibody served as controls. At least 50,000 cells per sample were acquired. Cardiac differentiation was quantified by the percentage of α-actinin-positive cells subtracted by negative control after gating out the dead cells. All of the data analyses were performed using the CellQuest software (Becton Dickinson).

***Preparation and Recellularization of Human Acellular Myocardial Slices & Cardiac Fibers*. Myocardial Slices:** To create acellular myocardial slices, full-thickness pieces of cardiac matrix were excised from the left ventricle of acellular human hearts (~2x2x2 cm^3), embedded in Tissue-Tek Optimal Cutting Temperature (O.C.T.) Compound (cat#: 4583; Sakura Finetek, Torrance, CA), and cryo-sectioned for 200-µm slices on a Leica CM3050 S cryostat (Leica Biosystems, Buffalo Grove, IL). Slices were carefully transferred to 6-well tissue culture plates and allowed to adhere at room temperature. OCT Compound was removed by a 5 min treatment with DI water, as the compound is water-soluble (per manufacturer protocol). Slices were sterilized with treatment of 100% ethanol, followed by successive PBS washing steps to rehydrate the matrix. Acellular slices were then primed with cardiomyocyte maintenance media (RPMI 1640, with B-27) for 12 hours. Each primed myocardial slice was seeded with 1.5×10^6 human iPS-derived cardiomyocytes (unsorted), which were allowed to adhere for 24 hours at 37°C. Cardiomyocyte maintenance media was changed every 2 days following the initial seeding period, spontaneously contracting tissue was observed 4-7 days after seeding, and functional tests were performed after 28 days in culture. **Cardiac Fibers:** Cardiac fiber bundles (15 mm length, 2.5 mm diameter) were cut from the left ventricular free wall of decellularized cardiac scaffolds, using sterile surgical tools and aseptic technique in a biological hood. Acellular fibers were then transferred to individual wells of a 12-well tissue culture plates, and then primed with cardiomyocyte maintenance media (RPMI 1640, with B-27; 2 mL per well) for 12 hours. Each primed cardiac fiber was then injected with 1.5×10^6 cardiomyocytes in 100 µL. Cell suspension that fell out or dripped off of the construct was collected after injection, and seeded with the cardiac fiber in a rotating bioreactor tube for an additional 12 hours (similar to methods published previously).[10] After the addition 12 hours of rotational bioreactor seeding, recellularized fibers were removed from the bioreactor tube with sterile forceps, and placed into 6-well tissue culture plates onto custom 22-gauge stainless steel posts (1.5 mm apart). Cardiomyocyte maintenance media was changed every 2 days following the initial seeding period, spontaneously contracting tissue was observed 7-10 days after seeding, and functional tests were performed after 30 days in culture.

***Mechanical Function of Human Cardiac Slices & Fibers.* Strain Analysis:** Strain of contracting myocardial slices and cardiac fibers was evaluated on successive image-stacks by using a high-spatial resolution sub-pixel algorithm called high density mapping[11], based on a method proposed by Foroosh and Zerubia[12]. This technique is partially based on the capabilities of conventional particle tracking or digital correlation techniques, displacements can be determined at hundreds of locations to provide a whole field measurement, with a demonstrated accuracy of 0.09 pixels and precision of 0.04 pixels[11, 13]. For myocardial slices, strain was assessed on both the cells (imaged using phase contrast, at the slice surface) and underlying ECM (imaged using autofluorescence in the GFP channel, 20 µm below the slice surface). Image stacks were acquired using a Nikon Eclipse TE200 microscope (Nikon, Melville, NY), with a 1280 x 1024 pixel resolution, at a frame rate of 20 fps for 20 seconds. For cardiac fibers, strain was assessed on deforming matrix 100-200 µm below the fiber surface, using a method called micro-optical coherence tomography (µOCT) to create image stacks at a frame rate of 40 fps for 30 seconds (µOCT method described below). For HDM analysis, all images were converted to 8-bit grayscale for analysis. Multiple contractions per sample were analyzed and averaged to determine area strain and frequency; Unpaced slices (n=6), paced slices (n=4), unpaced fibers (n=4). **Force analysis:** Contractile force was measured on submerged recellularized myocardial slices using an Aurora Scientific 403A Force Transducer system. Since myocardial slices were fixed to tissue culture plastic, force was measured by attaching a cantilever to the transducer, lowering the cantilever onto contractile cardiac tissue, and detecting uniaxial deflections (n=9). Cardiac fibers reseeded with iPS-derived cardiomyocytes were mounted lengthwise in our custom force measurement setup (**Supplemental Fig.VI**). Each fiber was placed in a warmed (37°C) media bath and one end was attached to a fixed point via a 6-0 silk suture. The other end was attached to a force transducer (403A Force Transducer system; Aurora Scientific) also via a 6-0 silk suture, with a preload of 50 mg (50 µN; n=4). In force measurements for both myocardial slices and cardiac fibers, the force transducer was calibrated with 10-, 50-, and 100-mg weights, and data was recorded at scale factor of 50 mg/volt. Signals were outputted to a PowerLab 16/35 digital acquisition device (cat. # PL3516, AD Instruments Inc., Colorado Springs, CO) with a sampling rate of 1 kHz, and then analyzed with LabChart software (cat. # MLU60/8, AD Instruments Inc.). **Electrical Stimulation During Mechanical Testing:** During stimulation for strain and force measurements, we studied the effects of electrical pacing. For myocardial slices, electrical pacing was conducted with a C-Pace EP system (30 V, 5 ms; IonOptix LLC, Milton, MA) with increasing frequencies: 1, 1.5, 2, 2.5, or 3 Hz. For cardiac fibers, electrical pacing was conducted with a Grass S88 Stimulator (30 V, 5 ms; Grass Technologies, Warwick, RI) with increasing frequencies: 1.5, 2, and 2.5 Hz.

Micro-Optical Coherence Tomography (µOCT). The use of µOCT in this paper was based on methods previously described.[14] Briefly, axial (z) ranging for OCT was achieved by intereferometric measurement of the optical delay of light returned from the sample. µOCT as implemented in this manuscript is based on Spectral-domain OCT (SD-OCT).[15] The application of µOCT in this setup employed very broad bandwidth light source (800±150 nm laser-generated supercontinuum) and a common path reference arm to achieve 1-µm depth or axial (z) resolution. To achieve high transverse resolutions, a high numerical-aperture objective lens (numerical aperture = 0.12) was used to focus the beam onto the sample. We further engineered the focus of the probe beam with an annular apodizer, which reduced the focal spot size from 2.4 to 2.0 µm. Apodization and chromatic dispersion extended the focal depth to ~250 µm, enabling cross-sectional imaging at high resolutions. The system operates with user-configurable line and frame rates and customizable scan geometry; settings were set to 40 frames per second, 512 A-lines per frame in a linear scan, and 0.5 mm by 0.5 mm (X by Z) for a cross-sectional image.

Cardiac Fiber Voltage Mapping. Recellularized cardiac fibers were treated with 20 mmol/L blebbistatin for 30 min to arrest motion, and then loaded with Di-8-ANEPPS (5 mmol/L) for 20 min at 37°C immediately prior to imaging. The cardiac fiber preparations were placed in a custom pacing and imaging chamber, and voltage mapping of cardiac electric activity was performed with this chamber and a charge-coupled device camera (CardioCCD-SMQ, RedShirt Imaging, Decatur, Ga) mounted on a Nikon TE2000 inverted microscope. The hearts were field paced at 60 bpm (Grass S48K Stimulator, West Warwick, RI). Samples were illuminated with a 120-W metal-halide Exfo X-Cite 120 lamp with a 480/40 nm excitation filter, and the fluorescence image was filtered through a 535/50 nm emission filter. Data were acquired at a frame rate of 125 Hz. NeuroPlex software (RedShirtImaging) was used to view image sequences and output darkfield-corrected mean fluorescence from regions of interest. Optical recordings were inverted and low-pass filtered at 100 Hz. Fluorophore photobleaching was subtracted using a custom program, and probe dynamics were fit using Clampfit software (Axon Instruments). Measurements of APDs were taken as the average of 3 successive beats for each sample (n=4). APD was calculated at 80% repolarization (APD80).

Human Heart Bioreactor. Whole-heart acellular scaffolds were cultured in the human heart bioreactor (**Figs. 4A,E**) which provides the organ with perfusion of media and mechanical stimulation. Perfusion was achieved by driving media from the organ chamber into the main coronary arteries. In parallel with the perfusion loop was a hollow-fiber oxygenator (Fiber oxygenator D150, cat. #73-3757, Harvard Apparatus, Holliston, MA) fed with carbogen gas (95% oxygen, 5% carbon dioxide) to maintain media buffering and oxygen content. The organ chamber also contained a small duct for collection of effluent from the coronary sinus (CS, not shown in Fig. 4A). Mechanical stimulation was delivered to the left ventricular wall via cyclic inflation and deflation of a fluid-filled balloon inserted into the LV via the mitral valve (**Fig. 4B**). Both perfusion pressure and LV pressure were monitored for the duration of culture (**Fig. 4F**). LV balloon inflation was controlled by oscillating the LV balloon pressure to deliver strain to the left ventricular wall (**Figs. 4B,C,F**). The entire setup was then placed within an incubator at 37°C to maintain physiologic temperature.

Preparation and Recellularization of Human Acellular Whole-Heart Scaffolds in the Human Heart Bioreactor. All preparations for whole-heart acellular scaffolds were performed using aseptic technique, sterilized tools, sterilized tubing, sterilized bioreactor parts, and sterile-filtered media. Whole-heart acellular scaffolds were prepared by dissecting down the aortic root to access the left main coronary artery (LCA), and then accessing the coronary sinus (CS) through the right atrium. Both the LCA and CS were cannulated. A latex balloon was inserted into the LV via the mitral valve, and prefilled to fill the ventricular cavity. The acellular scaffold was then mounted in the organ chamber of the bioreactor. The LCA cannula was attached to a perfusion line, the CS cannula was attached to a collection duct, and the LV balloon cannula attached to an external fluid reservoir behind the ventricle pump. Whole-heart acellular scaffolds were primed overnight with 1 L of cardiomyocyte maintenance media for 12 hours, at a rate of 60 mL/min, at 37°C. After priming, organ chambers were brought into a clean biological safety cabinet with laminar flow, whole-heart scaffolds were detached from the perfusion line, removed from the organ chamber, and placed in a sterile surgical pan. Primed scaffolds were seeded with ~500×10^6 human iPS-derived cardiomyocytes (unsorted) by intra-myocardial injection, into the epicardial surface of the left ventricular free wall, between the LAD and left circumflex coronary artery (LCX; **Fig. 4D**). Recellularized whole-heart scaffolds were then reattached to the perfusion line, the organ chamber was sealed and returned back to the 37°C incubator, and cells attached under static culture for 3-4 hours. After the static period, perfusion culture was started at 20 mL/min for the first 12 hours, and then increased to 60 mL/min on day 2. Media volume was increased to 1.5 L at the beginning of static culture, and changed every 48 hours. Functional tests were performed after 14 days in culture. Six hearts were recellularized and cultured in this fashion, which are listed Supplemental Table I.

Functional analysis of Human Acellular Whole-Heart Scaffolds. **Metabolic Analysis:** Pre-perfusion media samples were collected from freshly prepared RPMI/B-27, prior to adding it to the bioreactor for coronary circulation. Post-perfusion media samples were collected via the coronary sinus duct tubing, every 48 hours (just before the next media exchange). Media samples were analyzed using an i-STAT®1 Analyzer (cat. # 04P75-01, Abbot Laboratories Inc., Abbot Park, IL) with CG8+ and CG4+ i-STAT cartridges (cat. #s 03P88-25 and 03P85-25, respectively, Abbot Laboratories Inc.). **Epicardial Force Measurement:** As defined intramyocardial regions were difficult to isolate without compromising whole-heart scaffolds, contractile force was measured on recellularized whole-hearts using a method similar to that used on recellularized myocardial slices. Briefly, a cantilever was attached to an Aurora Scientific 403A Force Transducer system, which was then lowered onto contractile cardiac tissue to detect uniaxial deflections. **LV Pressure Development:** Left ventricular pressure traces were obtained using a calibrated pressure transducer (cat. #: SPR-671; Millar, Inc., Houston, TX) that was guided through a pilot port and inserted into the lumen of the LV balloon. The LV balloon was then prefilled to an isovolumetric pressure of 20 mmHg, and pressure fluctuations were recorded within the closed volume. The pressure transducer signals were recorded using a Transducer Amplifier Module (cat. # D-79232, Hugo Sachs Elektronik / Harvard Apparatus, Holliston, MA), using a 150 Hz high-pass filter and a 0.1 Hz low-pass filter. Pressure signals were outputted to a PowerLab 16/35 digital acquisition device (cat #: PL3516; AD Instruments Inc., Colorado Springs, CO), and then analyzed with LabChart software (cat #: MLU60/8; AD Instruments Inc.). **Electrical Pacing, ECG, and Electrical Activation Mapping:** Electrical pacing was conducted with a Grass S88 Stimulator (10-80 V, 5 ms, at 0.8 Hz; Grass Technologies, Warwick, RI) and implanted temporary cardiac pacing wires (cat. # TPW50, Ethicon, Somerville, NJ) located at the border of the recellularized volume. Electrocardiograms were recorded using an ECG Amplifier System and micro-electrodes (cat. # D-79232, Hugo Sachs Elektronik / Harvard Apparatus, Holliston, MA), using a 150 Hz high-pass filter and a 0.1 Hz low-pass filter. ECG signals were outputted to a PowerLab 16/35 digital acquisition device (cat #: PL3516; AD Instruments Inc., Colorado Springs, CO), and then analyzed with LabChart software (cat #: MLU60/8; AD Instruments Inc.). For electrical activation mapping, a custom plaque electrode was constructed from an 8x8 PGA socket with gold/nickel plating (cat. #: 522-13-064-08-000001; Mill-Max Manufacturing Corp., Oyster Bay, NY) to create an 8x8 pin array with 2.54 mm spacing between pins. Each socket in the 8x8 pin array was coupled to an input on a Prucka Engineering CardioLab Amplifier (GE Healthcare, Wilmington, MA). The 8^{th} row of pins in each column were designated as reference channels, and electrical signals were recorded with a CardioLab 4000 EP Recording System (GE Healthcare, Wilmington, MA), with a sampling rate of 1 kHz, and using a 150 Hz high-pass filter and a 0.1 Hz low-pass filter.

Force and Pressure Trace Analysis. Force generation traces acquired from recellularized myocardial slices, fibers, and recellularized whole-hearts were processed using custom Python scripts using SciPy[16-18] to extract pulse amplitudes, periods, time to X% relaxation, and dominant frequency. A set of approximately 8-12 pulses were analyzed per biological sample per condition and extracted parameters were averaged within a set to obtain representative values. Amplitudes were calculated as the absolute value between baseline and pulse peak. Periods were calculated as the time distance between consecutive pulse peaks. Time to X% relaxation was calculated as the time distance between pulse peak and the signal amplitude reducing by X% of peak amplitude. Dominant frequency was measured by first calculating a fast-Fourier transform of the pulse set and then choosing the frequency corresponding to the highest peak in the frequency domain. Left ventricular pressure traces from recellularized whole-hearts were also processed using custom Python scripts to extract pulse peak pressure, maximum & minimum dP/dt, and tau. Pulse peak pressure was calculated as the absolute value between baseline and pulse peak. Maximum & minimum dP/dt was calculated as the maximum & minimum values of the derivative of the pressure trace with respect to time within one pulse period. Tau was calculated by fitting an exponential decay equation to the pressure trace between minimum dP/dt and the start of the next pressure pulse.[19]

Transmission Electron Microscopy. Tissue was fixed in Karnovsky fixative of 2.5% glutaraldehyde plus 2% paraformaldehyde and stored overnight at 4°C. Tissue was washed of fixative in 0.1 M sodium cacodylate buffer (pH 7.2) then postfixed in 2% OsO4 in sodium cacodylate buffer, dehydrated in a graded alcohol series, and embedded in Epon t812 (Tousimis, Rockville, MD). Ultrathin sections were cut on a Reichert-Jung Ultracut E microtome (Vienna, Austria), collected on uncoated 100-mesh copper grids, stained with uranyl acetate and lead citrate, and examined on a Philips CM-10 transmission electron microscope (Eindhoven, The Netherlands).

Statistical Analysis. Results for coronary flow, vascular resistance, and biochemical analysis are presented as mean ± standard deviation (SD). Results for mechanical testing of myocardium are presented as mean ± standard deviation (SD). Comparisons for coronary flow and vascular resistance we performed using a 2-way analysis of variance (ANOVA) for solution type and cause of death, followed by the Tukey post hoc comparison test. Comparisons for biochemical analysis and biaxial testing on myocardium were performed using a student's t-test. In all tests, differences were considered statistically significant at a value of $p < 0.05$. Data for area strain and force-curve metrics of myocardial slices are represented as mean ± standard deviation, and comparisons were performed using a 2-way ANOVA with a Tukey post hoc test for unstimulated versus stimulated conditions. All plots (except for Fig. 3J) were generated using the Python 2D plotting library matplotlib[20].

For each study, preliminary data analysis or pilot experimentation was performed to determine the magnitude of the effect between study groups and this data was used to perform a power analysis to calculate sample size requirements. The sample size for animal studies was based on sample sizes used for similar studies, previously described in the literature.[21] As a pre-established criteria triaged by the NEOB, donor hearts with a known medical history of coronary artery disease were excluded from our study. Randomization was based on the availability of decellularization chambers and acquisition of donor tissue. For example, if the decellularization chambers were occupied, the donor tissue was allocated into the control group. No randomization methods were employed for animal studies. Based on the processing technique utilized to prepare the samples, blinding was not incorporated into the analysis of the experiments, nor was it incorporated in animal studies.

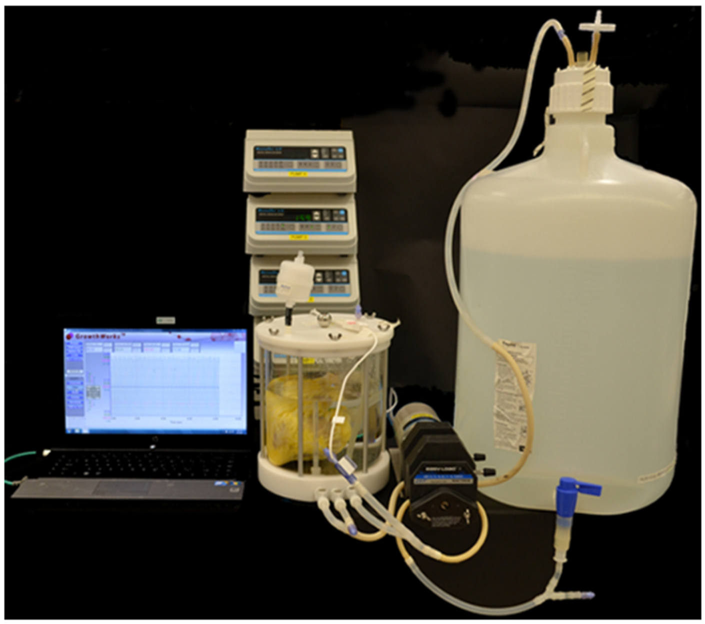

Supplemental Figure I
Photograph of the perfusion decellularization setup. From left to right: Laptop running pump control software, pump controllers, chamber containing a human heart undergoing the decellularization process, roller pump, 50L carboy fluid reservoir.

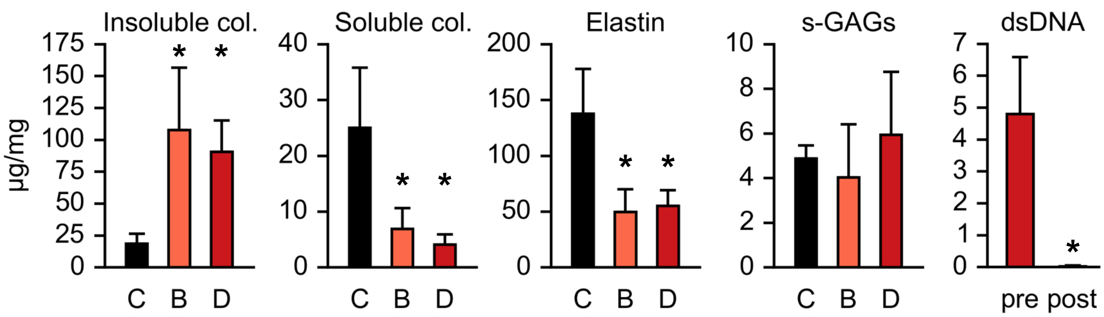

Supplemental Figure II

Biochemical analysis for insoluble collagen (hydroxyproline), soluble collagen, α-elastin, and sulfated glycosaminoglycans (s-GAGs) on normal cadaveric human myocardium (C, n = 5 hearts), decellularized human cardiac matrix from hearts donated after brain death (B, n = 4), and decellularized human cardiac matrix from hearts donated after cardiac death (D, n = 4). Three tissue samples were analyzed per heart per component and the average of those three was used as the representative value for the component in that heart. Normalized to tissue dry weight. Error bars are standard de viation. Asterisks (*) indicate $p < 0.05$ compared to cadaveric condition.

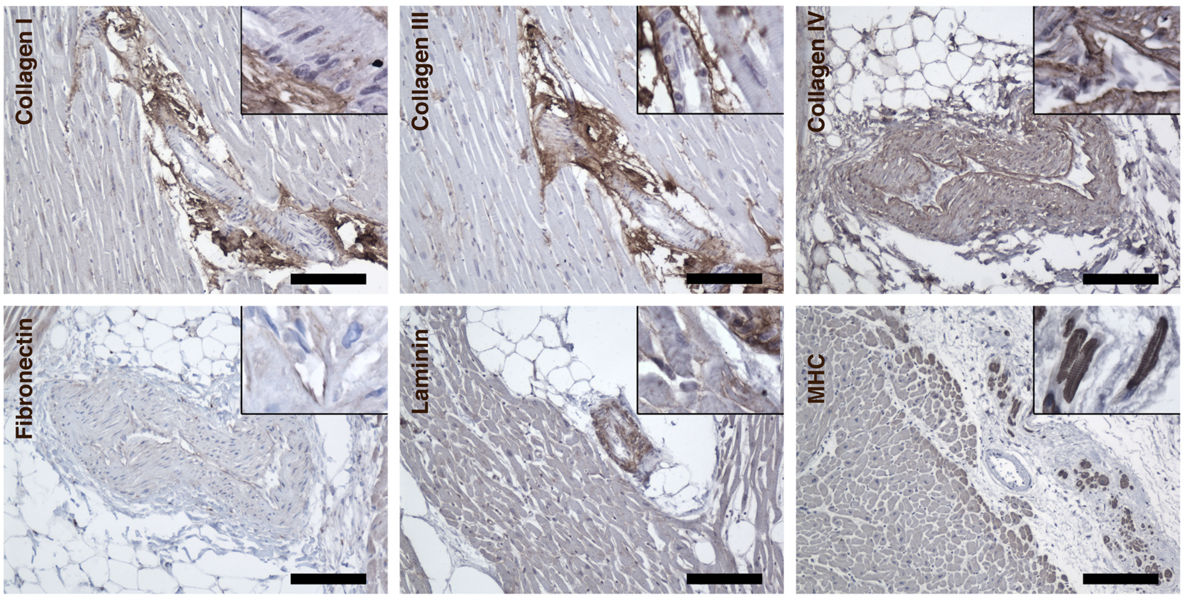

Supplemental Figure III

Immunohistochemical staining of cadaveric myocardium for collagens I, III, IV, fibronectin, laminin, and myosin heavy chain (MHC). Scale bar, 200 µm.

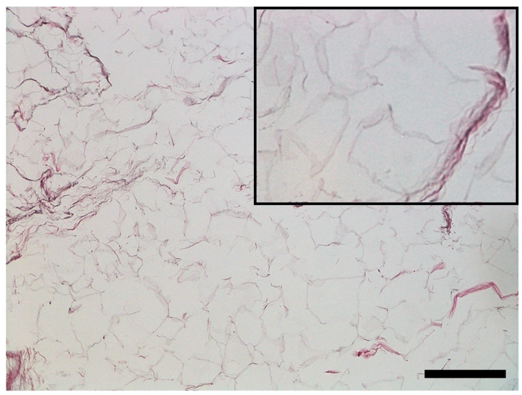

Supplemental Figure IV
Adipose tissue matrix remaining after the decellularization process. Scale bar, 100 µm.

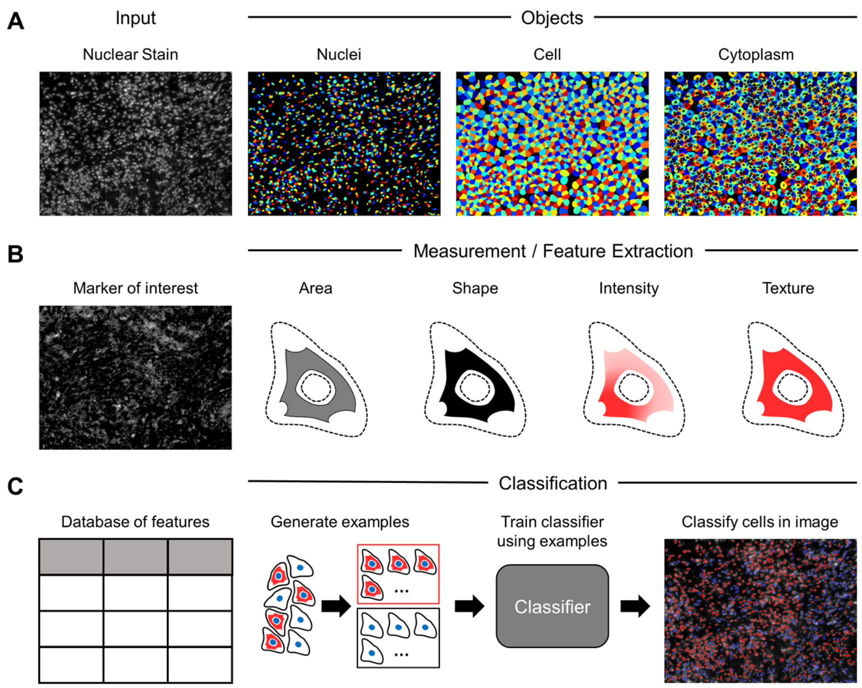

Supplemental Figure V
Quantification of cell markers (CD68, CD80, CD163) using CellProfiler and CellProfiler Analyst.

A. Grayscale images of a nuclear stain (DAPI) are read into CellProfiler (www.cellprofiler.org) and nuclei objects are identified. Nuclei objects are propagated outwards by a specified distance (20 pixels) to obtain cell objects. Cytoplasm objects are then generated by subtracting nuclei objects from cell objects. Nuclei, cell, and cytoplasm objects share a one-to-one relationship.

B. Corresponding images of the marker(s) of interest are overlaid on the nuclei, cell, and cytoplasm objects. Various area, shape, intensity, and texture features are extracted per object for each object class and stored in a SQLite database. To extract these features, a CellProfiler pipeline was used based on: Jones TR, et al. *Proc Natl Acad Sci U S A*. 2009 Feb 10;106(6):1826-31. Features are extracted for all markers of interest within an image (e.g. CD68 only, CD68 with CD80, or CD68 with CD163).

C. Image thumbnails of the identified and measured objects are then presented to the user/researcher who generates an example set of positive and negative cells (a training set). Using CellProfiler Analyst, a classifier is then trained with this set and subsequently used to score all of the cells identified in the input images. The output is the number of cells belonging to each class (positive or negative, red or blue overlay respectively in example) per image.

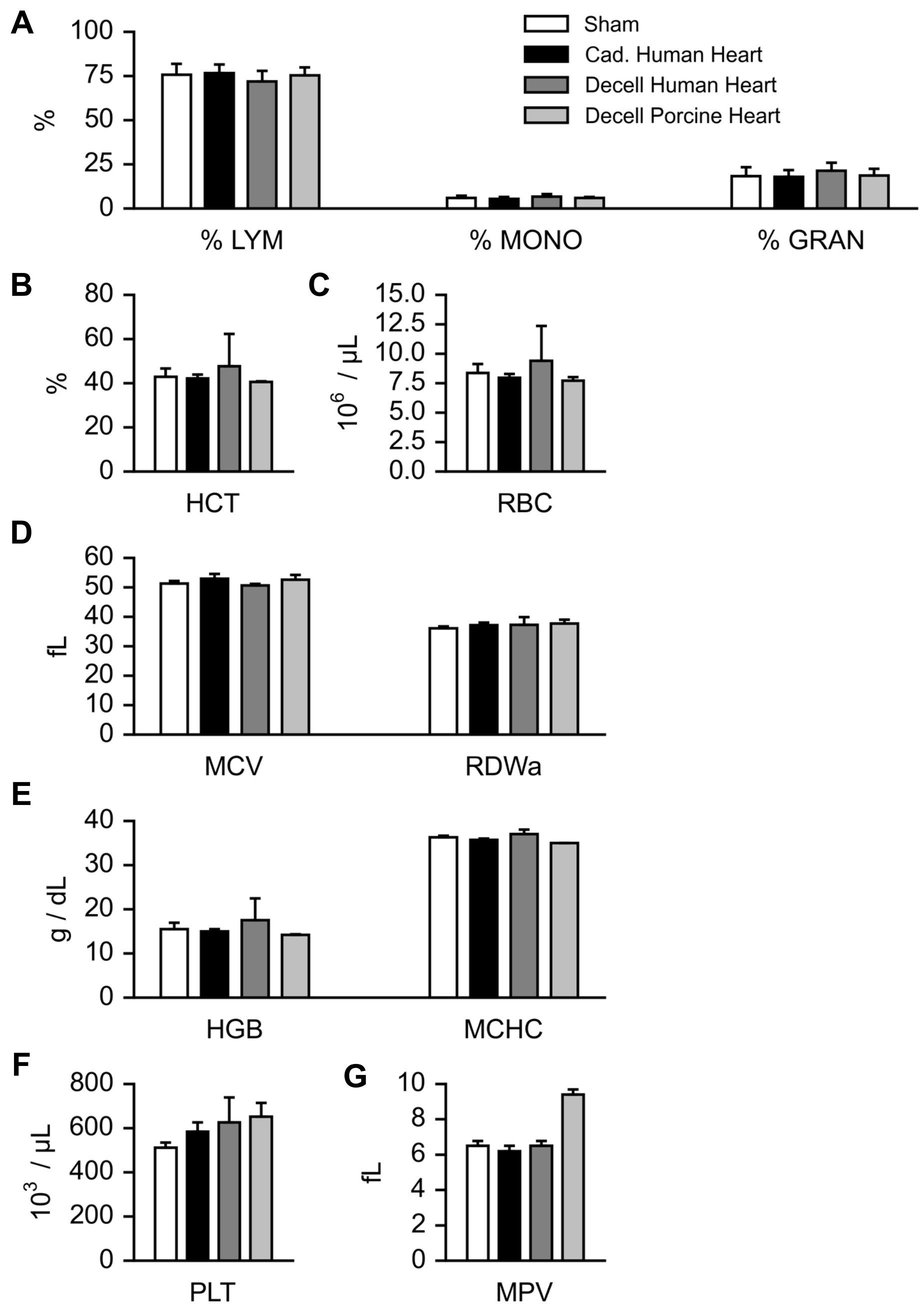

Supplemental Figure VI
White blood cell (WBC) component percentages (n = 3 rats per condition). Error bars are standard deviation. fL, femtoliters.

A. Sub-populations of WBCs as a percentage of total WBCs. LYM, lymphocytes; MONO, monocytes; GRAN, granulocytes
B. HCT, hematocrit
C. RBC, red blood cells
D. MCV, mean cell volume of RBCs; RDWa, red cell width
E. HGB, hemoglobin concentration; MCHC, mean cell hemoglobin concentration
F. PLT, total platelet count
G. MPV, mean platelet volume

Decellularized HH without coronary artery disease

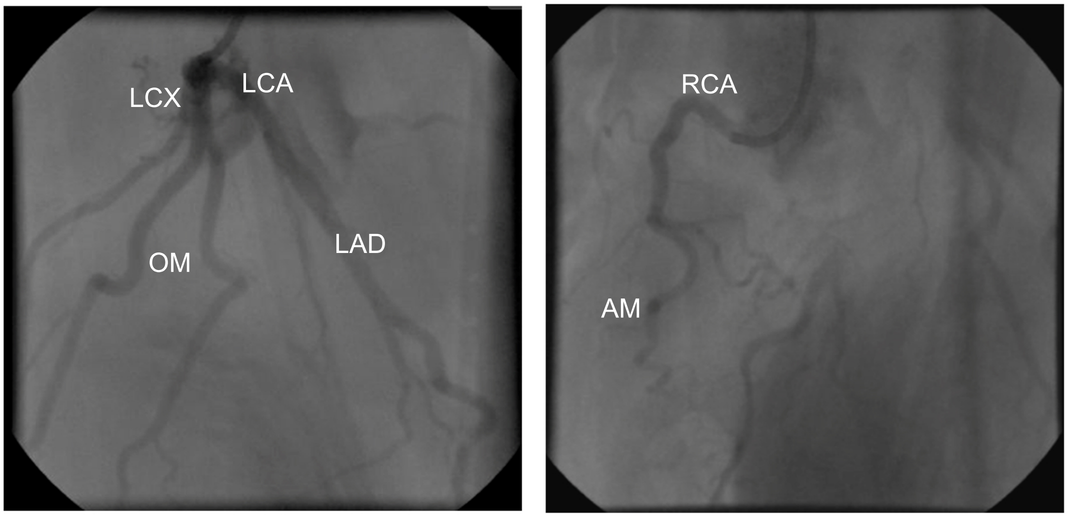

Decellularized HH with coronary artery disease

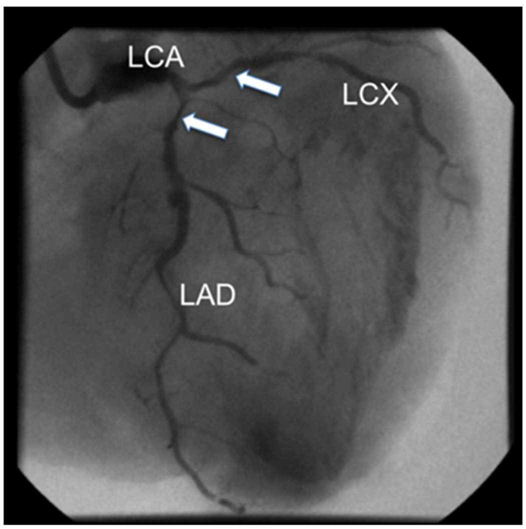

Supplemental Figure VII

Top: Coronary angiography of left and right main coronary arteries in decellularized human hearts. Left coronary artery (LCA), left anterior descending artery (LAD), left circumflex artery (LCX), obtuse marginal artery (OM), right coronary artery (RCA), acute marginal artery (AM).

Bottom: Angiography of an acellular heart from a patient presenting with coronary artery disease. White arrows indicate luminal narrowing related to atherosclerotic plaques.

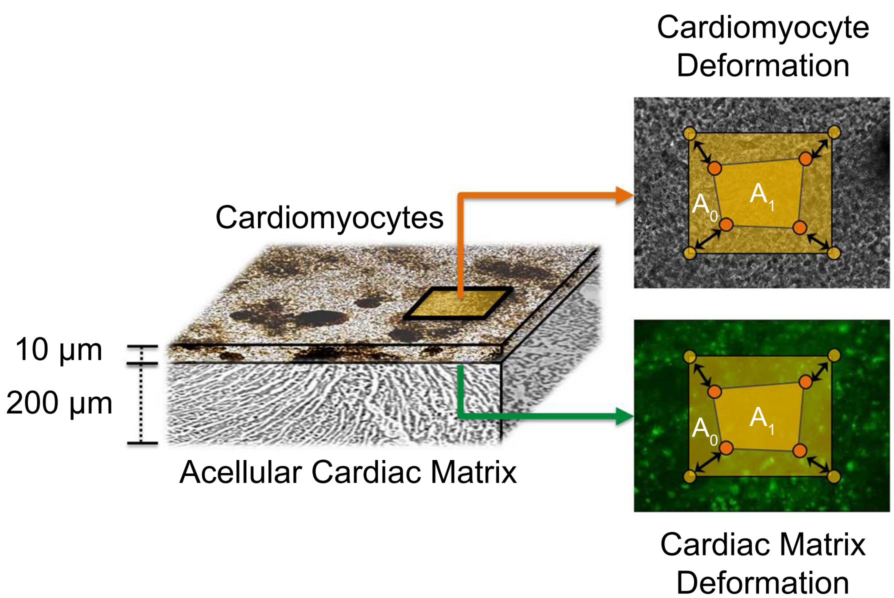

Supplemental Figure VIII

Schematic of HDM analysis for area strain of matrix-seeded human cardiomyocytes and underlying cardiac matrix.

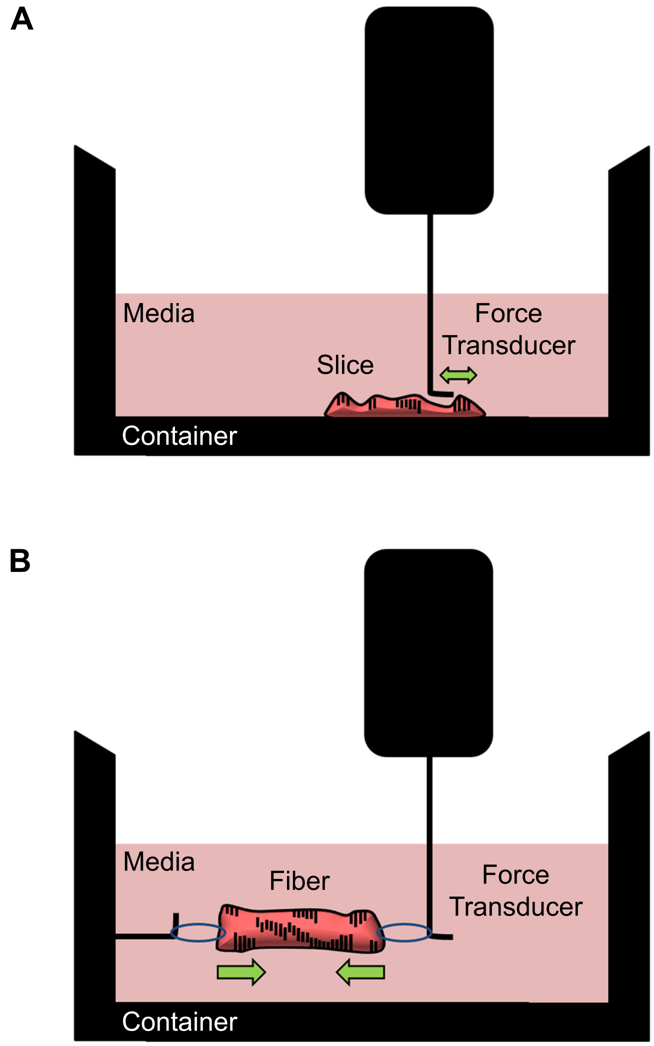

Supplemental Figure IX

A. Schematic depicting setup for measuring force generation in reseeded cardiac slices. The slice is attached to the container while the force transducer is brought into contact with contractile nodules. Green arrows indicate axis of nodule contractility.

B. Schematic depicting setup for measuring force generation in reseeded cardiac fibers. The left hook is fixed while the right hook is free-moving and attached to the force transducer. Green arrows indicate axis of fiber contractility.

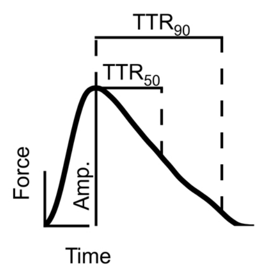

Supplemental Figure X
Schematic of force-curve metrics illustrating amplitude, time to 50% relaxation (TTR_{50}), and time to 90% relaxation (TTR_{90}).

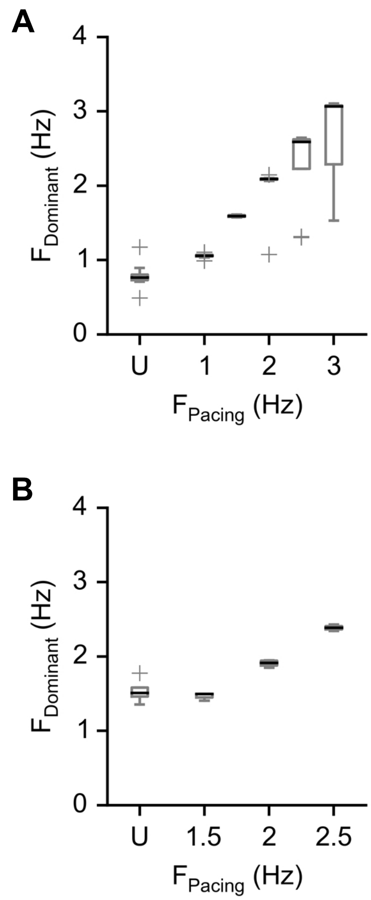

Supplemental Figure XI

Captured frequencies of reseeded cardiac slices (A) and reseeded cardiac fibers (B) under unpaced (U) and paced conditions.

Supplemental Table I. Donor heart data

Heart ID	Decell, Control	Sex M, F	Cause of Death DCD, DBD	Age yrs.	Height cm	Weight kg	BMI kg/m^2	Experimental Allocation
1	D	NA	***	***	***	***	***	Establishment of the perfusion decellularization process; Matrix histology
2	D	M	B	36	177.80	86.18	27.20	Establishment of the perfusion decellularization process; Matrix histology; Biochemical analysis; Sterility testing
3	D	M	B	72	177.80	105.69	33.40	Establishment of the perfusion decellularization process; Matrix histology
4	C	NA	***	***	***	***	***	Matrix histology
5	D	M	B	41	170.18	98.88	34.22	Refinement of perfusion decellularization; Flow/Resistance analysis; Matrix histology; Sterility testing
6	D	F	C	52	160.02	76.20	29.80	Refinement of perfusion decellularization; Flow/Resistance analysis; Matrix histology; Sterility testing
7	C	NA	***	***	***	***	***	Biochemical analysis; DNA content; Matrix histology; Biaxial mechanical testing
8	D	M	C	57	185.42	115.21	33.46	Flow/Resistance analysis; Biochemical analysis; DNA content; Proteomics
9	D	M	B	52	177.80	90.72	28.31	Flow/Resistance analysis; Matrix histology; Sterility testing
10	C	M	B	61	177.80	118.39	37.45	Biochemical analysis; DNA content; Biaxial mechanical testing
11	D	F	C	47	162.56	69.85	26.49	Flow/Resistance analysis; Biochemical analysis; DNA content; Proteomics; Sterility testing
12	D	M	B	57	170.18	83.91	28.97	Flow/Resistance analysis; Biochemical analysis; DNA content; Proteomics; Biaxial mechanical testing; Sterility testing
13	D	NA	***	***	***	***	***	Flow/Resistance analysis; Sterility Testing
14	C	M	B	44	167.64	67.13	23.84	Matrix histology; Matrix mechanics
15	C	M	C	58	177.80	78.93	24.90	Vascular histology; Matrix mechanics
16	D	F	C	48	162.56	70.76	26.83	Flow/Resistance analysis; Biochemical analysis; DNA content; Proteomics
17	C	M	C	47	167.64	99.79	35.43	Flow/Resistance analysis; Biochemical analysis; Matrix mechanics
18	C	M	B	67	165.10	64.86	23.88	Biaxial mechanical testing; Biochemical analysis; Matrix histology
19	D	F	B	64	157.48	132.90	53.63	Flow/Resistance analysis; Biochemical analysis; DNA content; Proteomics
20	D	M	B	73	172.72	59.87	20.11	Biaxial mechanical testing
21	C	M	B	59	187.96	120.66	34.10	Biochemical analysis; DNA content
22	D	M	C	56	177.80	89.36	28.22	Biochemical analysis; Biaxial mechanical testing
23	D	M	B	53	182.88	99.79	29.90	Biochemical analysis; Biaxial mechanical testing
24	C	M	B	51	165.10	67.13	24.39	Vascular histology; Matrix mechanics
25	C	M	B	18	175.26	73.03	23.78	Biaxial mechanical testing
26	C	F	B	64	157.48	59.42	24.10	Biaxial mechanical testing
27	D	F	B	73	162.56	67.13	25.46	Flow/Resistance analysis; Matrix mechanics
28	D	F	B	59	162.56	113.85	43.14	Biaxial mechanical testing
29	D	F	B	78	165.10	63.96	23.48	Vascular analysis by angio
30	D	F	B	56	152.40	54.88	23.81	Vascular analysis by angio
31	D	F	B	64	160.02	83.01	32.37	Sterility testing
32	C	M	B	50	175.26	91.17	29.74	Vascular analysis by angio; Matrix mechanics
33	C	M	B	56	165.10	69.85	25.61	Vascular analysis by angio; Matrix mechanics
34	C	F	C	65	170.18	57.15	19.68	Micro-vascular analysis with contrast dye; Matrix mechanics
35	C	F	C	45	172.72	77.11	25.78	Micro-vascular analysis with contrast dye
36	D	M	C	50	185.42	84.82	24.67	Sterility testing; Recellularization (436.4 million cells); Perfusion culture; Force-generating contraction testing; Histology

37	C	F	B	72	165.10	89.81	33.46	Micro-vascular analysis with micro-beads; Matrix mechanics
38	C	F	B	76	162.56	83.46	31.52	Micro-vascular analysis with micro-beads; Matrix mechanics
39	C	F	B	72	177.80	74.84	23.72	Micro-vascular analysis with iron particles
40	C	M	C	52	177.80	71.21	22.46	Micro-vascular analysis with Microfil®
41	C	M	C	61	172.72	88.45	29.71	Micro-vascular analysis with Microfil®
42	D	F	B	47	160.02	75.30	29.33	Biaxial mechanical testing
43	C	M	C	24	185.42	142.43	41.83	Vascular analysis by angio
44	C	F	B	29	170.18	99.79	34.52	Biaxial mechanical testing
45	D	F	B	56	157.48	49.90	20.16	Matrix slice recellularization
46	D	M	C	26	180.34	69.85	21.52	Matrix slice recellularization
47	D	F	C	66	182.88	104.33	31.22	Matrix slice recellularization
48	D	M	C	21	185.42	63.50	18.47	Sterility testing; Recellularization (467.2 million cells); Perfusion culture; Force-generating contraction testing; Ventricular pressure development testing; Histology
49	C	F	C	58	160.02	68.95	26.88	Biaxial mechanical testing
50	D	M	B	26	177.80	74.84	23.72	Sterility testing; Recellularization (520.1 million cells); Biomimetic culture; Ventricular pressure development testing; Histology; Reseeded volume assessment (27.97%)
51	C	F	C	25	180.34	107.05	33.02	RNA/Histology controls
52	D	M	C	38	185.42	119.75	34.77	Sterility testing; Recellularization (513.7 million cells); Biomimetic culture; Metabolic analysis; Force-generating contraction testing; Histology
53	C	F	C	67	167.64	72.12	25.82	RNA/Histology controls
54	C	M	C	55	177.80	91.17	28.85	RNA/Control cell isolation
55	D	F	B	33	175.26	74.84	24.37	Matrix slice recellularization
56	C	F	B	66	162.56	66.22	24.98	RNA/Control cell isolation
57	D	M	B	58	193.04	84.82	22.56	Sterility testing; Matrix fiber recellularization
58	D	F	C	62	165.10	64.86	23.88	Sterility testing; Matrix fiber recellularization
59	D	M	B	49	180.34	80.29	24.72	Biaxial mechanical testing
60	C	F	B	51	154.94	62.60	26.12	Biaxial mechanical testing
61	D	M	B	57	172.72	77.11	25.73	Sterility testing; Matrix fiber recellularization
62	D	M	C	55	165.10	67.13	24.61	Sterility testing; Recellularization (485.6 million cells); Biomimetic culture; Ventricular pressure development testing; Electrophysiology testing; Histology; Reseeded volume assessment (32.53%)
63	C	F	C	58	172.72	76.20	25.48	Immunological response study
64	D	F	B	59	160.02	49.90	19.53	DNA content; Immunological response study
65	D	F	B	61	162.56	59.87	22.71	Sterility; Recellularization (562.3 million cells); Biomimetic culture; Ventricular pressure testing; Electrophysiology testing; Histology; Reseeded volume assessment (50.17%)
66	D	NA	***	***	***	***	***	Sterility testing
67	D	F	B	51	172.72	60.78	20.35	Micro-vascular analysis with Microfil®
68	C	F	B	24	154.94	49.90	20.69	Micro-vascular analysis with Microfil®
69	C	M	C	45	185.42	118.84	34.61	Proteomics; Matrix Histology
70	D	M	C	51	177.80	94.80	30.05	Sterility testing; Matrix fiber recellularization
71	D	M	C	28	170.18	74.84	25.89	Proteomics; Matrix Histology
72	C	M	C	55	162.56	73.03	27.62	Proteomics; Matrix Histology
73	C	F	C	58	162.56	70.31	26.52	Proteomics; Matrix Histology
	Decell: 40 Control: 33	M: 36 F: 32	DCD: 29 DBD: 39	52.43 ± 14.29	170.96 ± 9.53	81.54 ± 20.53	27.76 ± 6.09	DCD - donation after cardiac death, DBD - donation after brain death, NA - Not Available; Highlighted hearts were recellularized.

Supplemental Table II. Decellularized Myocardium Peptide List

Decellularized Unique Proteins				***Spectral Counts***		***Normalized Relative Abundance***	
Accession	***Peptide count***	***Unique peptides***	***Confidence score***	*Average*	*St.Dev.*	*Average*	*St.Dev.*
FBN1_HUMAN	114	109	9904.63	140.0	42.9	1134459622.73	113563050.71
CO4A2_HUMAN	19	19	2460.61	30.5	16.7	392909648.31	204818539.63
PGBM_HUMAN	75	75	7029.81	77.2	32.4	173234761.32	79209570.13
ALBU_HUMAN	39	39	3214.59	45.0	14.0	93995455.22	22667320.51
CO4A1_HUMAN	13	11	1403.38	13.0	8.0	88725437.86	68364377.64
LAMC1_HUMAN	44	44	3922.51	45.5	19.8	77874517.83	34795554.75
CO1A2_HUMAN	6	6	739.61	9.3	2.1	57691467.21	38304993.53
CO6A3_HUMAN	53	53	3620.71	46.7	2.8	57040103.92	10328972.57
LAMB2_HUMAN	45	44	3265.47	39.5	15.1	40323169.36	7013367.30
CO1A1_HUMAN	11	11	669.65	7.3	3.7	37615581.18	22165708.19
LAMA2_HUMAN	58	58	3845.32	40.7	26.9	26730050.04	13352495.51
CILP1_HUMAN	11	11	768.48	10.2	2.7	23633730.01	4960837.89
SAMP_HUMAN	6	6	437.31	6.0	0.6	20298689.22	3104574.42
MYH7_HUMAN	57	56	3736.39	38.5	20.7	17121399.11	11082852.12
FINC_HUMAN	27	27	1620.67	18.3	2.7	13022664.19	7210508.05
LAMB1_HUMAN	35	34	2271.76	23.0	12.1	10916579.09	4939717.03
CO6A2_HUMAN	11	11	636.04	8.8	2.3	10251159.58	7288349.36
CO6A1_HUMAN	11	11	982.91	11.5	1.0	9752546.73	2716022.36
LAMA5_HUMAN	34	34	2053.05	23.8	11.1	8265030.58	2971613.06
AMBP_HUMAN	8	8	622.88	6.0	2.8	7469426.22	2723317.28
MFAP2_HUMAN	2	2	171.19	1.8	1.0	7071690.33	2885558.93
VTNC_HUMAN	9	9	569.26	8.5	5.6	6845741.61	4350939.33
MYG_HUMAN	8	8	629.84	7.7	4.5	5952768.86	3927977.02
FBLN2_HUMAN	9	9	676.01	8.8	5.3	5878464.78	2346330.34
FIBG_HUMAN	8	8	433.50	3.8	1.0	5423399.53	6957620.89
CO5A3_HUMAN	2	2	110.45	1.7	0.8	4965755.81	3166135.70
EMIL1_HUMAN	15	15	922.56	9.8	6.8	4836736.76	6679099.14
IGKC_HUMAN	5	5	642.50	6.5	4.5	4429234.91	2908278.66
MFAP5_HUMAN	4	4	326.96	4.2	0.8	4032517.47	819970.49
FBLN3_HUMAN	11	11	809.37	6.3	3.8	3847198.28	1370414.33
TGM2_HUMAN	4	4	222.29	2.8	1.2	3807822.04	4657576.70
FHL2_HUMAN	8	8	469.15	4.2	3.5	3519248.78	2589215.79
MYL3_HUMAN	6	6	382.08	4.7	4.2	3408789.25	2627481.39
TIMP3_HUMAN	5	5	278.14	4.8	3.9	3241670.07	2371628.18
TPM1_HUMAN	10	7	824.93	4.7	4.3	3157494.14	2444111.41
ACTA_HUMAN	11	4	679.29	2.7	1.2	3140768.20	2092546.71
EMIL3_HUMAN	3	3	136.44	2.2	0.4	3092769.12	1565337.97
TITIN_HUMAN	52	52	2607.61	19.3	25.1	2985047.58	3194076.38
IGHG1_HUMAN	8	4	556.69	3.8	2.3	2980569.66	218906.81
FBLN5_HUMAN	9	9	457.08	6.0	2.4	2965564.64	826387.14
FABPH_HUMAN	7	7	405.70	3.8	2.3	2870557.06	1999161.38
HBB_HUMAN	5	5	413.58	5.3	1.2	2814557.57	2546396.38
CSPG2_HUMAN	9	9	753.48	8.2	5.2	2240995.81	237278.79
LDB3_HUMAN	9	9	620.10	4.7	4.6	2222835.35	1619079.00
LUM_HUMAN	8	8	494.19	7.3	3.5	1878572.90	689315.57
MLRV_HUMAN	7	7	372.94	4.3	2.9	1878335.55	1338712.33
ACTG_HUMAN	11	4	771.65	1.7	0.5	1874289.91	2178446.07
BGH3_HUMAN	5	5	291.70	4.2	2.3	1806924.49	711985.03
TRFE_HUMAN	11	11	585.45	5.2	3.9	1778840.14	799749.52
HBA_HUMAN	3	3	150.24	2.0	1.5	1737273.80	1153257.67
FHL1_HUMAN	4	4	205.06	1.7	1.0	1735646.86	853480.58
DCD_HUMAN	3	3	195.98	2.0	0.6	1701191.96	920201.13
THSD4_HUMAN	8	8	380.23	5.5	1.4	1645757.40	1066703.86
PGS2_HUMAN	3	3	155.93	2.3	1.2	1513594.38	615280.62
KCRM_HUMAN	6	6	335.17	4.0	2.7	1467889.88	1062579.49
CO8A1_HUMAN	4	4	196.51	2.3	1.9	1421496.20	329543.12

NID1_HUMAN	12	10	717.88	7.2	1.9	1418056.35	361864.33
DEF1_HUMAN	2	2	81.15	0.8	1.3	1294704.05	745804.08
DESM_HUMAN	7	6	459.47	3.3	2.7	1255126.46	904383.57
TENX_HUMAN	8	8	408.70	3.8	2.1	1210271.29	1466079.79
ACTN2_HUMAN	14	10	779.50	4.5	5.1	1096251.57	946458.86
LDHB_HUMAN	4	3	209.40	1.8	1.6	1081138.29	1255579.63
DESP_HUMAN	15	15	714.06	6.0	4.9	1058153.91	882337.06
EMIL2_HUMAN	3	3	186.79	1.7	1.4	1044015.56	451779.63
FBN2_HUMAN	6	2	450.28	0.7	0.8	1032494.64	1137230.53
G3P_HUMAN	5	5	305.60	3.2	2.3	1020150.86	917179.35
ATPA_HUMAN	6	6	352.09	4.0	2.8	1018732.74	442714.28
FLNA_HUMAN	4	4	173.66	2.8	2.2	939750.54	426080.81
NID2_HUMAN	7	6	372.99	2.5	1.4	918812.78	180029.44
FBLN1_HUMAN	4	4	183.06	1.7	1.2	839379.81	198465.44
NPNT_HUMAN	4	4	180.65	2.2	2.0	826376.08	621585.44
ADT1_HUMAN	5	5	228.14	2.7	0.5	809191.41	537089.84
EF1A2_HUMAN	3	3	179.40	1.8	1.2	807001.41	912786.32
FIBA_HUMAN	3	3	140.43	1.8	1.0	738941.21	897967.47
DAND5_HUMAN	2	2	172.45	3.2	2.5	724917.12	563120.56
CSRP3_HUMAN	2	2	115.68	1.2	1.5	711830.81	467164.75
LTBP1_HUMAN	4	4	224.42	2.5	0.8	661821.29	165524.43
HSPB6_HUMAN	2	2	75.40	0.7	1.0	649178.01	958503.40
PDLI5_HUMAN	6	6	310.82	3.2	3.0	646156.22	653402.22
TSP4_HUMAN	4	4	180.37	1.8	0.8	636212.58	163572.94
ATPB_HUMAN	5	5	270.71	2.3	1.2	593105.51	410581.22
MFAP4_HUMAN	2	2	116.29	1.2	1.2	573380.74	674810.14
TNNT2_HUMAN	4	4	206.07	2.2	2.3	572443.67	521655.11
PTGDS_HUMAN	3	3	260.42	2.5	2.0	564175.58	276841.71
CO3_HUMAN	9	9	456.03	5.5	2.4	545527.66	232431.62
POSTN_HUMAN	8	8	448.02	3.7	0.8	541336.40	502617.84
MFGM_HUMAN	5	5	263.00	2.3	2.9	537076.82	572638.67
FIBB_HUMAN	3	3	166.05	1.3	0.5	519143.16	611350.01
ODO2_HUMAN	2	2	81.54	1.8	1.2	479863.43	385724.17
KCRS_HUMAN	5	5	361.19	2.3	2.2	468363.55	357113.89
HSP7C_HUMAN	3	3	182.53	1.8	1.2	445748.14	444074.62
IGHA1_HUMAN	4	4	278.55	2.3	2.2	437976.70	268764.42
MDHC_HUMAN	3	3	153.71	1.8	1.2	435107.50	397476.37
SRBS2_HUMAN	4	4	196.92	2.2	2.6	414832.84	542214.03
MDHM_HUMAN	4	4	214.16	2.2	1.7	413716.38	340224.14
ITIH1_HUMAN	2	2	99.67	0.7	1.0	413424.58	589136.52
COLA1_HUMAN	2	2	104.18	1.0	0.9	411518.08	199301.96
TINAL_HUMAN	4	4	250.49	1.8	1.6	411319.86	321478.88
TNNC1_HUMAN	4	4	175.82	2.2	2.4	395744.49	374252.75
CO4A3_HUMAN	3	2	203.90	1.0	0.9	395648.84	284166.58
ACON_HUMAN	5	5	284.16	2.0	1.8	383863.74	311518.42
AACT_HUMAN	4	4	200.76	2.2	0.8	381401.79	264040.48
CO9_HUMAN	3	3	157.36	1.7	1.4	373139.96	320761.93
COCA1_HUMAN	3	3	193.11	2.2	1.7	353756.26	185065.66
CBPA3_HUMAN	5	5	268.59	2.3	2.3	338067.52	347095.66
ELN_HUMAN	2	2	104.14	0.8	1.3	332289.62	490245.22
LYSC_HUMAN	4	4	238.30	2.5	1.4	329591.23	157009.98
KPYM_HUMAN	2	2	104.42	0.7	0.8	320242.60	220362.81
CRYAB_HUMAN	3	3	197.68	1.7	1.9	310610.00	284958.83
COIA1_HUMAN	2	2	141.37	0.5	0.5	300927.19	201407.22
CO4A4_HUMAN	2	2	102.68	1.7	0.5	297698.18	35710.17
RS27A_HUMAN	2	2	103.40	1.3	0.8	273093.52	98845.03
S10A8_HUMAN	3	3	143.19	2.0	0.6	265138.83	117495.15
AATC_HUMAN	3	3	148.15	1.5	1.4	261136.29	285900.55
C1QB_HUMAN	2	2	92.09	1.3	1.0	233300.22	178967.62

CISY_HUMAN	3	3	176.97	1.3	1.0	233286.33	195335.88
H4_HUMAN	3	3	181.55	1.5	0.5	228775.76	190323.46
CMA1_HUMAN	4	4	184.42	2.2	1.8	226940.40	219996.45
DERM_HUMAN	2	2	252.78	1.8	1.6	225281.55	185242.98
PGS1_HUMAN	3	3	159.07	1.7	1.6	224981.76	152205.79
TPIS_HUMAN	4	4	252.77	1.8	1.5	220638.19	164620.11
ATL4_HUMAN	2	2	97.27	1.0	0.9	208976.52	217956.95
SAP_HUMAN	2	2	72.85	1.2	0.4	205667.59	222385.95
ALDOA_HUMAN	2	2	123.39	1.0	0.0	197886.13	175366.40
VDAC1_HUMAN	4	4	254.41	1.8	1.3	192493.62	145396.41
1433T_HUMAN	2	2	81.84	1.2	0.8	189351.93	136041.32
COFA1_HUMAN	4	4	216.71	2.5	1.2	178476.71	43909.49
HEMO_HUMAN	4	4	164.10	2.0	1.3	176310.56	24733.16
S10A9_HUMAN	2	2	122.02	1.3	1.0	175597.79	108151.23
MYPC3_HUMAN	3	3	175.15	1.5	0.5	173998.03	121955.34
FLNC_HUMAN	5	5	234.17	1.5	2.0	153428.88	90055.86
MYOZ2_HUMAN	2	2	86.08	0.5	0.8	133080.55	116144.11
COSA1_HUMAN	4	4	187.23	2.0	1.9	130769.13	100544.07
AOC3_HUMAN	4	4	159.31	2.0	1.8	130039.32	78375.13
HSPB1_HUMAN	2	2	88.84	1.3	0.5	125040.56	121791.32
PLAK_HUMAN	5	4	377.29	1.5	2.3	123049.02	170244.38
CO4B_HUMAN	2	2	81.14	0.7	0.5	121139.91	115390.67
MYH10_HUMAN	3	2	133.17	0.8	0.4	116013.70	58682.89
PRELP_HUMAN	3	3	167.98	1.3	1.4	114585.11	76245.71
WNT2B_HUMAN	2	2	148.31	1.7	1.4	114450.60	104794.67
PRDX6_HUMAN	3	3	149.14	2.2	1.3	113436.74	102548.39
SDF1_HUMAN	2	2	102.01	1.3	1.0	108005.83	70025.60
S10A7_HUMAN	2	2	83.43	1.2	0.8	101343.43	70942.79
VINC_HUMAN	3	3	135.40	1.0	1.5	95236.46	124814.05
VDAC2_HUMAN	2	2	98.73	0.8	1.0	90389.36	63634.94
CTNB1_HUMAN	4	3	194.24	0.8	1.3	88372.90	128259.64
IDHP_HUMAN	2	2	87.62	0.7	1.0	81168.96	63768.29
ANXA2_HUMAN	2	2	100.73	1.0	0.6	77119.46	15924.58
ASPN_HUMAN	3	3	151.43	1.3	1.0	75426.50	46353.33
CO4A5_HUMAN	4	2	389.90	1.0	0.0	67806.73	23632.94
ECM1_HUMAN	2	2	91.94	0.7	0.5	62456.43	73007.52
ADH1B_HUMAN	3	3	128.16	0.8	1.3	60925.34	61095.13
HPLN1_HUMAN	2	2	163.77	1.2	1.0	59810.09	51965.44
PPIA_HUMAN	2	2	82.67	0.5	0.5	54416.10	43693.12
ETFB_HUMAN	2	2	93.67	0.5	0.8	52111.80	52699.77
A2MG_HUMAN	2	2	100.14	1.2	1.0	49957.26	14469.71
VIME_HUMAN	3	2	150.86	0.8	0.4	46230.72	37880.84
PLEC_HUMAN	5	5	234.49	1.7	2.6	45892.70	69309.68
COEA1_HUMAN	2	2	107.17	0.8	1.0	44703.39	12671.62
MYOM1_HUMAN	2	2	102.93	0.7	1.0	39608.93	20661.81
MYOM2_HUMAN	2	2	102.59	0.5	0.8	18298.29	27462.88
ACADV_HUMAN	2	2	94.48	0.7	1.0	14303.97	22430.82

Supplemental Table III. Cadaveric Myocardium Peptide List

Cadaveric Unique Proteins				***Spectral Counts***		***Normalized Relative Abundance***	
Accession	***Peptide count***	***Unique peptides***	***Confidence score***	*Average*	*St.Dev.*	*Average*	*St.Dev.*
MYH7_HUMAN	207	61	22334	94.2	10.6	1854575662.79	628397285.59
MYL3_HUMAN	14	12	1447.81	19.7	3.2	1231120573.43	306612860.04
TITIN_HUMAN	892	886	63390.64	787.2	75.5	1153003445.10	420215261.86
MYG_HUMAN	15	15	2097.59	30.8	3.8	911754840.71	357883463.84
MLRV_HUMAN	23	22	1888.1	34.0	2.8	816283949.65	167636791.27
ALBU_HUMAN	40	40	3358.48	49.5	6.0	600583340.49	398831601.05
ACTN2_HUMAN	52	33	4733.75	43.3	2.6	529661082.52	116470483.59
HBA_HUMAN	7	7	533.82	9.2	4.7	525622887.36	463577092.84
KCRM_HUMAN	17	16	1329.27	16.7	2.6	445722331.08	115906289.75
FABPH_HUMAN	12	11	1059.39	15.3	2.5	407336289.62	143603773.66
TPM1_HUMAN	31	13	3208.73	22.8	2.4	357578925.61	95768016.59
DESM_HUMAN	37	30	2823.84	29.7	4.8	296016112.63	95657251.17
TNNC1_HUMAN	9	9	640.35	8.2	2.2	290778199.92	32058834.15
TNNT2_HUMAN	16	16	1404.97	19.7	4.2	267183886.78	69024475.72
ATPB_HUMAN	25	24	2263.85	29.8	4.0	264567874.74	86391064.78
KCRS_HUMAN	18	17	1606.19	18.3	3.9	252761362.05	59267865.72
MYPC3_HUMAN	56	55	4471.75	56.3	6.5	238963210.81	64545652.30
ACON_HUMAN	32	32	3077.83	37.0	2.8	238604118.92	96694854.61
ATPA_HUMAN	21	21	1639.34	23.0	2.4	238474035.74	91332222.17
MDHM_HUMAN	15	15	1416.41	18.8	1.6	228192925.22	54459026.13
HBB_HUMAN	12	6	1192.38	8.8	2.8	218933580.06	212200777.07
G3P_HUMAN	14	14	1359.43	20.5	2.5	202699396.66	50038286.22
TNNI3_HUMAN	13	11	822.38	11.3	1.6	182841865.43	34371794.76
MDHC_HUMAN	9	9	926.83	12.0	1.7	169243364.65	54488729.24
ALDOA_HUMAN	19	18	1429.76	17.7	2.9	115832106.71	35481954.60
CRYAB_HUMAN	10	10	868.25	12.8	2.5	112415463.70	19526271.57
CISY_HUMAN	11	11	747.08	11.5	1.9	110430482.19	34864746.82
IDHP_HUMAN	23	20	1714.67	21.7	2.1	107479796.67	58588930.16
CYC_HUMAN	9	9	679.14	11.8	1.6	106803087.30	30292759.05
LDHB_HUMAN	16	14	1184.44	13.2	3.1	104571577.82	43809906.27
ECHA_HUMAN	27	27	1812.57	25.7	2.3	94557599.42	15327145.50
MYOM2_HUMAN	55	55	4197.01	51.7	2.0	91209727.71	28291217.56
QCR2_HUMAN	10	10	1059.83	13.3	1.0	77065570.44	29954136.46
ECHB_HUMAN	23	23	1681.64	22.3	3.1	75930072.61	14154919.82
FLNC_HUMAN	66	59	5125.22	51.7	8.9	74964682.03	26011636.61
ACADV_HUMAN	27	27	2172.69	27.7	3.3	74453483.72	14150846.46
TPIS_HUMAN	12	12	1148.07	14.0	1.5	69778596.34	22314727.79
NNTM_HUMAN	26	26	1850.75	26.7	1.5	68572600.73	27119366.53
KPYM_HUMAN	15	15	1380.61	16.8	2.3	67203754.73	17437252.34
THIL_HUMAN	11	11	1037.42	12.3	3.8	64856093.06	13901850.63
AATC_HUMAN	15	15	998.75	14.3	1.9	64847121.18	22672319.97
MYOM1_HUMAN	51	51	4114.2	49.2	2.1	63683350.67	18212481.55
FHL2_HUMAN	20	20	1606.26	23.7	3.1	62265570.33	21456031.10
DECR_HUMAN	9	9	592.85	7.5	2.1	61652815.16	28558475.54
ETFB_HUMAN	13	13	1085.2	14.0	2.1	61013137.93	19138343.82
AATM_HUMAN	17	17	1110.85	16.8	2.1	60896255.80	16958683.73
COX5B_HUMAN	6	6	626.32	6.5	2.1	60885659.81	16946596.83
QCR1_HUMAN	12	11	989.14	11.3	2.5	57109883.04	22271251.60
SDHA_HUMAN	17	17	1501.37	17.3	1.9	56214836.13	19111502.41
COX41_HUMAN	10	10	682.73	9.8	1.9	54994746.63	10581661.57
DLDH_HUMAN	11	11	963.6	11.3	2.0	54677044.13	24160875.56
COX5A_HUMAN	8	8	629.76	8.7	1.2	50428742.23	9702224.71
PGK1_HUMAN	20	20	1352.9	19.7	2.2	49053907.55	13445781.91
ACADM_HUMAN	13	13	903.7	12.7	1.8	47878012.38	5701309.02
MPCP_HUMAN	9	9	419.43	7.5	1.2	47865120.84	22022743.86
SPTN1_HUMAN	69	69	4703.14	60.5	8.6	47299085.60	9859465.39

AT2A2_HUMAN	24	24	1978.1	21.0	3.7	46831382.30	20214695.82
ATPO_HUMAN	7	7	484.84	7.2	2.2	45587923.25	23734875.29
CH60_HUMAN	24	24	1485.33	20.7	3.1	42509009.34	3101949.18
LDB3_HUMAN	20	20	1416.63	18.2	1.2	40907964.17	4966998.24
ETFA_HUMAN	11	11	914.29	10.7	2.5	40560630.26	12410439.20
HSPB1_HUMAN	9	9	910.87	14.0	2.5	40206974.38	11418200.71
VINC_HUMAN	29	29	2222.95	25.5	2.2	40105929.47	7649098.60
VDAC1_HUMAN	11	9	838.42	8.8	1.8	39466585.00	10418463.01
COX2_HUMAN	3	3	132.51	2.5	0.8	36291374.54	18515738.32
ODPA_HUMAN	14	14	919	12.2	1.3	35820086.28	9788911.58
GRP75_HUMAN	19	19	1713.55	19.7	2.4	34616780.20	3735102.86
PEBP1_HUMAN	10	10	870.69	11.3	2.2	34323049.61	9993846.09
VDAC2_HUMAN	10	9	911.74	9.7	1.6	34165315.33	7486498.89
GRP78_HUMAN	21	20	1836.22	19.7	3.8	33732834.86	11290804.35
ADT1_HUMAN	15	5	1023.71	6.7	1.4	33460347.74	9993113.65
ODO1_HUMAN	29	28	2135.69	25.5	4.4	32946781.01	12901644.34
COX6C_HUMAN	7	7	447.66	7.8	2.8	31656691.17	11412031.20
NDUS1_HUMAN	21	21	1351.57	18.7	3.4	31562490.68	9004970.17
ATP5H_HUMAN	7	7	650.67	8.7	1.2	31222089.74	7473206.66
ALDH2_HUMAN	18	16	1165.14	14.5	1.8	29743750.86	10380757.43
H4_HUMAN	8	8	654.35	9.3	2.3	29518050.67	11666105.25
ODO2_HUMAN	8	8	512.79	5.8	1.0	29335170.74	1162981.80
CATD_HUMAN	9	9	617.9	9.5	1.9	29229702.49	5649646.14
THIM_HUMAN	13	13	771.66	11.2	2.6	28226866.89	13807959.74
HCDH_HUMAN	9	9	649.93	8.3	1.8	27719095.79	6414690.76
PARK7_HUMAN	9	9	617.56	8.0	1.4	27428360.24	5423314.31
HPT_HUMAN	16	16	1180.67	11.7	10.5	27239148.96	32112478.02
ECH1_HUMAN	10	10	636.94	8.5	1.0	27053753.04	2237630.11
PPIA_HUMAN	8	8	593.68	8.3	2.0	26905540.17	7225156.12
ODPB_HUMAN	10	10	963.34	10.7	2.6	26904838.48	11986182.11
VIME_HUMAN	25	18	1687.36	14.3	1.6	26450525.34	4868836.77
ATPG_HUMAN	8	8	529.42	8.2	1.8	26390728.75	11907819.42
NDUV1_HUMAN	15	15	1095.31	15.2	2.6	25925576.65	5970994.55
MIC60_HUMAN	22	21	1593.21	18.2	2.1	25885797.82	6729671.07
ATPD_HUMAN	3	3	239.08	3.2	0.8	25782130.47	9738204.41
PGAM2_HUMAN	10	5	790.07	5.7	1.4	25468404.15	6319462.73
HSP7C_HUMAN	23	15	1869.21	16.5	4.2	25245199.76	9028937.59
LMNA_HUMAN	25	24	1596.78	17.5	2.5	25024989.82	1694821.60
TRFE_HUMAN	23	23	1469.2	17.8	2.0	24879236.14	17396000.61
FBN1_HUMAN	42	40	2764.31	30.8	7.8	24426214.64	9667372.55
CSRP3_HUMAN	8	8	658.67	6.7	1.5	23711392.71	11684385.65
PRDX1_HUMAN	12	11	701.96	10.0	2.4	23193325.57	6319800.64
FUMH_HUMAN	12	12	783.95	9.8	2.0	22854087.71	12509345.83
ATP5J_HUMAN	5	5	699.86	6.0	2.9	22592046.44	22583868.61
ATP5L_HUMAN	5	5	520.76	7.0	0.6	22146742.98	6311263.06
PRDX5_HUMAN	8	8	753.68	9.7	3.7	21903910.48	12811441.83
PRDX2_HUMAN	7	6	459.36	6.8	1.3	21869152.87	7213635.87
ETFD_HUMAN	12	12	836	9.8	1.9	21751268.99	6957765.20
ALDOC_HUMAN	13	12	943.81	11.2	2.4	21654048.50	5703606.12
CO6A3_HUMAN	40	39	2150.7	30.2	2.8	21559243.25	6803778.73
HSDL2_HUMAN	16	16	1050.09	12.3	2.5	21375691.35	8220109.61
ACBP_HUMAN	9	9	744.01	9.5	1.6	21223290.27	4958680.04
MYOM3_HUMAN	33	33	2406.95	29.0	5.0	20780416.12	8699829.78
SUCA_HUMAN	5	5	380.07	4.8	1.2	20517843.61	10974676.63
ECHM_HUMAN	10	10	815.04	10.2	2.1	20212443.95	7302453.61
PRDX3_HUMAN	9	9	632.29	8.3	2.0	19441342.41	3567211.70
SDHB_HUMAN	9	9	871.57	10.0	1.3	19348395.34	3768484.62
AIFM1_HUMAN	16	16	964.48	11.8	2.3	19114296.64	4723406.32
ACTN1_HUMAN	23	6	2066.09	7.7	2.5	18915597.41	9439025.88

ODP2_HUMAN	12	11	761.99	10.3	1.5	18905076.01	3614193.80
AT5F1_HUMAN	9	9	577.03	8.3	1.6	18656052.79	6499375.91
SPTB2_HUMAN	50	45	3189.71	35.7	2.6	18411233.76	2691792.23
KCRB_HUMAN	10	9	821.67	10.3	1.6	18184264.80	6211327.13
HS71A_HUMAN	16	10	1114.55	9.8	0.8	18107743.24	3031470.71
ATP5I_HUMAN	4	4	202.97	4.2	1.5	18000962.16	4882968.36
ANXA6_HUMAN	17	17	1265.38	15.7	2.1	17636805.13	3728770.56
SRCH_HUMAN	9	9	1304.45	14.8	1.9	17241545.76	5979042.30
LAMC1_HUMAN	28	28	1840.48	21.5	3.5	17201029.07	5469476.06
KAD1_HUMAN	6	6	408.75	6.3	1.2	16960731.65	9672275.69
CH10_HUMAN	6	6	368.96	5.5	1.0	16841863.77	2944806.79
DMD_HUMAN	40	39	2305.67	28.0	5.6	16736991.98	4873670.17
PGBM_HUMAN	44	44	2722.11	32.7	4.5	16584451.72	576444.06
G6PI_HUMAN	8	8	609.14	7.8	1.5	16458202.99	4349357.15
IGKC_HUMAN	3	3	409.35	4.2	1.7	16243977.87	4421834.80
ENOB_HUMAN	14	11	1079.29	11.7	3.6	16146251.36	3311467.82
SUCB1_HUMAN	9	9	513.99	8.0	1.5	16058038.66	7888000.33
PRDX6_HUMAN	9	9	549.84	8.5	3.1	15981688.10	5127377.87
SODM_HUMAN	6	6	478.29	6.2	0.8	15644558.36	2729489.64
FHL1_HUMAN	8	8	483.74	5.8	1.2	15573643.24	841566.94
H31T_HUMAN	3	3	117.53	2.5	0.5	15442826.21	6200365.97
MYOZ2_HUMAN	7	7	563.3	6.8	2.5	15375897.10	5096248.68
UCRI_HUMAN	5	5	229.1	3.2	1.0	15267246.21	5410139.08
CY1_HUMAN	3	3	376.43	5.0	1.5	15213497.93	5154703.58
GELS_HUMAN	12	11	966.09	12.7	1.8	15158891.90	1508886.19
SCOT1_HUMAN	7	7	535.68	6.7	1.2	15130263.24	10096422.40
IGHG1_HUMAN	7	4	486.6	4.0	0.9	14850730.27	2216914.15
PDLI5_HUMAN	12	12	776.85	11.3	2.0	14777409.84	487655.52
LEG1_HUMAN	3	3	263.97	3.0	0.9	14760709.35	3491779.67
SRCA_HUMAN	13	13	1130.6	14.0	4.4	14701934.00	5142748.84
ACSL1_HUMAN	17	16	958.53	13.7	1.6	14683909.20	3120871.70
CASQ2_HUMAN	8	7	543.15	7.5	1.0	14646121.63	3085792.60
PHB_HUMAN	8	8	431.87	6.5	0.8	14605026.57	3402302.48
NDUS2_HUMAN	9	9	465.43	8.3	1.2	14395940.87	4153095.49
SRBS2_HUMAN	12	11	629.89	7.7	2.2	14329005.95	4438072.12
H2AZ_HUMAN	3	3	125.52	2.2	1.0	14243750.20	5432318.02
PFKAM_HUMAN	15	12	1171.21	11.8	2.1	14241924.00	1473006.90
MYL4_HUMAN	11	8	945.75	8.2	4.3	13794721.80	13665481.00
NEBL_HUMAN	19	18	1110	15.0	2.5	13792852.48	3647200.49
PLEC_HUMAN	54	53	2930.55	39.7	6.0	13589272.99	4984922.48
USMG5_HUMAN	4	4	424.85	5.5	1.2	13242426.37	4118975.11
QCR7_HUMAN	6	6	336.65	5.2	1.2	13003641.63	3059145.69
HSPB6_HUMAN	5	5	385.08	6.3	1.2	12973944.73	2983427.66
LAMA2_HUMAN	39	39	2453.58	28.7	4.3	12873899.56	3103045.69
XIRP1_HUMAN	31	30	1690.71	21.2	7.0	12700350.88	7075656.44
PDIA1_HUMAN	16	16	1058.29	15.0	1.8	12375618.11	1466144.13
CMC1_HUMAN	18	18	936.41	12.5	1.5	12306125.95	2808107.18
NIPS2_HUMAN	5	4	357.57	4.8	1.9	12196057.30	3655593.44
TGM2_HUMAN	10	10	767.32	9.3	1.9	12173535.97	2427431.74
ACTC_HUMAN	26	4	2691.57	7.5	2.1	12118176.69	7545032.98
3HIDH_HUMAN	7	7	837.86	8.8	0.8	12062623.48	2467276.95
LDHA_HUMAN	9	7	613.93	6.7	2.0	12062261.52	4521927.34
COQ9_HUMAN	2	2	324.19	2.2	0.8	12058852.32	2381317.13
A1AT_HUMAN	12	10	697.8	8.5	0.8	11948656.79	7208264.17
ANXA2_HUMAN	13	13	804.95	13.7	2.3	11896744.63	2853462.87
NDUV2_HUMAN	9	9	695.53	8.3	0.8	11786741.16	3061252.60
NDUA4_HUMAN	3	3	145.27	2.5	0.8	11779921.26	7019019.10
CX6B1_HUMAN	4	4	306.42	4.2	1.3	11558910.83	7766095.88
KAD3_HUMAN	7	7	540.03	8.8	2.0	11551375.70	3467937.12

MYH6_HUMAN	155	17	15602.32	11.0	9.0	11410618.16	10913929.67
CO6A1_HUMAN	13	12	1049.48	12.5	1.9	10961783.11	4439084.48
NDUBA_HUMAN	7	7	376.46	6.3	1.4	10929724.58	3670774.10
ECI1_HUMAN	5	5	464.85	6.2	1.5	10910697.52	2506518.43
NDUB9_HUMAN	6	6	399.62	4.7	1.6	10793511.21	2493148.38
MIC19_HUMAN	6	6	515.75	6.2	1.2	10768828.53	2373786.20
TERA_HUMAN	17	17	1020.43	12.5	1.2	10505732.98	2830207.66
1433E_HUMAN	14	11	1026.4	11.2	2.3	10319061.33	2549299.30
FIBB_HUMAN	11	11	738.89	8.7	4.3	10140592.84	7225437.36
PDIA3_HUMAN	14	14	773.99	12.0	3.5	9932780.70	1248563.92
NDUA9_HUMAN	8	8	394.38	6.5	1.4	9847586.30	3642668.93
NDUS6_HUMAN	3	3	270.95	2.8	0.8	9843046.68	2768383.53
NDUA7_HUMAN	7	7	430.4	5.7	2.3	9792591.59	2687104.28
NDUBB_HUMAN	2	2	89.67	1.7	0.5	9671053.47	3853648.97
HS90A_HUMAN	20	10	1290.41	8.2	0.8	9654315.69	1213270.18
DHE3_HUMAN	13	13	791.38	10.5	1.9	9588313.87	3007006.71
HS90B_HUMAN	21	12	1254.31	9.2	1.2	9558615.74	2058065.68
MMSA_HUMAN	15	15	879.71	12.3	4.8	9483813.16	6224701.33
ALDR_HUMAN	7	6	379.49	5.2	1.0	9453050.95	2938151.71
GPD1L_HUMAN	10	9	559.76	6.8	1.6	9360949.52	6223633.23
CALM_HUMAN	4	4	238.47	4.8	1.0	9357599.30	2742369.65
GSTO1_HUMAN	8	8	410.77	6.8	1.8	9333662.18	3356637.24
NDUS5_HUMAN	6	6	392.84	5.2	1.0	9223719.91	3813173.18
LAMB2_HUMAN	28	25	1828.42	20.2	3.5	9075782.96	3073210.17
CPT1B_HUMAN	12	12	704.43	9.5	2.4	9053996.40	3749905.47
CAV1_HUMAN	3	3	148.43	2.0	0.6	8999523.03	2980787.80
VDAC3_HUMAN	7	5	467.27	5.0	0.9	8931699.66	1281153.58
HXK1_HUMAN	17	16	928	12.3	3.0	8833926.91	2057261.84
NDUAD_HUMAN	6	6	381.55	4.8	1.7	8782975.12	3277090.67
PGAM1_HUMAN	10	5	786.45	5.5	1.0	8588684.15	2401216.65
NDUB7_HUMAN	5	5	316.69	5.8	0.4	8373699.42	209243.94
CO6A2_HUMAN	8	8	491.44	7.2	1.3	8263898.69	1544891.54
FABP5_HUMAN	8	8	586.41	6.0	0.9	8220891.01	3681897.80
FABP4_HUMAN	4	3	235.86	2.8	0.8	8093734.58	2033533.99
NB5R3_HUMAN	6	6	316	4.5	1.9	8021052.17	1811794.87
NDUAA_HUMAN	8	8	570.21	7.7	1.2	7806255.51	4266911.57
CATB_HUMAN	7	6	481.13	5.8	1.5	7702209.68	1986614.06
CALR_HUMAN	10	10	623.31	8.5	1.4	7664279.78	2409983.74
NDUA2_HUMAN	6	6	500.81	5.5	1.4	7608920.29	1753827.09
PPIF_HUMAN	4	4	178.05	2.3	1.0	7585180.18	1447794.01
ENOA_HUMAN	9	8	794.36	8.3	1.4	7558895.06	396503.83
PHB2_HUMAN	8	8	520.36	6.5	1.8	7490986.89	1820456.58
TPM2_HUMAN	19	4	1861.85	3.5	2.2	7283297.20	2162188.25
NDUA5_HUMAN	5	5	350.12	4.8	0.8	7223900.34	961810.16
S10A6_HUMAN	2	2	79.89	1.7	0.5	7210978.45	2493476.17
RINI_HUMAN	11	11	753.62	8.2	0.8	7202311.81	1373958.69
NDUB3_HUMAN	4	4	165.03	3.3	0.8	7036856.08	1470380.39
PGM1_HUMAN	8	8	446.92	6.2	1.2	7030431.62	1454277.90
CALX_HUMAN	9	9	685.66	9.0	1.4	6938344.94	1968235.80
CO3_HUMAN	23	22	1158.24	14.8	4.7	6867807.74	3695835.06
KAD2_HUMAN	7	7	401.23	4.7	1.0	6834917.13	1576802.27
IGHA1_HUMAN	5	5	335.69	3.8	1.6	6808506.12	3038932.55
CISD1_HUMAN	3	3	245.31	3.2	1.2	6800548.68	2228361.61
PYGB_HUMAN	18	13	964.61	10.7	1.6	6692930.73	837902.07
QCR8_HUMAN	4	4	245.36	4.2	1.2	6688888.01	3150028.37
ANXA5_HUMAN	6	6	288.66	4.8	1.6	6646748.61	2788568.06
PTRF_HUMAN	8	8	755.76	7.5	2.3	6644887.08	1585846.11
MYH9_HUMAN	25	22	1623.8	15.7	4.7	6602480.47	2075683.92
FLNA_HUMAN	31	27	1991.72	19.8	2.6	6597602.64	1106564.07

ACOT1_HUMAN	8	8	446.53	5.3	0.8	6576500.70	3861030.89
ASAH1_HUMAN	6	6	259.53	4.2	1.0	6557031.70	1521885.73
EF2_HUMAN	12	12	750.08	9.5	2.3	6521596.07	692811.80
DESP_HUMAN	28	28	1442.19	18.2	2.4	6463057.54	612810.71
IGHG2_HUMAN	6	2	314.99	1.7	0.5	6380822.26	2403450.64
ACTS_HUMAN	25	3	2329.18	3.7	1.2	6277224.07	3109689.74
SLMAP_HUMAN	11	11	594.15	8.2	2.1	6200956.25	1623490.04
AHNK_HUMAN	36	36	1967.23	18.5	12.7	6033743.64	3509527.64
AT1B1_HUMAN	5	5	368.65	5.0	1.7	6019239.86	909913.41
ACADS_HUMAN	8	8	606.79	6.8	1.5	5973280.53	2171606.68
HEMO_HUMAN	7	7	434.65	5.0	1.3	5951004.05	5448321.03
FIBG_HUMAN	9	9	673.47	6.7	2.4	5867230.17	3530690.55
AL4A1_HUMAN	8	8	499.85	6.3	1.4	5699815.68	2567611.94
RT36_HUMAN	5	5	556.37	7.5	2.3	5589813.19	2876121.74
CYTB_HUMAN	3	3	315.23	4.0	1.3	5530407.36	2958280.16
NDUS3_HUMAN	8	8	503.53	6.5	1.5	5497883.55	2290110.18
PGM5_HUMAN	8	8	520.93	6.2	1.7	5471351.74	1585077.08
1433Z_HUMAN	7	4	426.84	2.8	1.0	5465791.50	885491.80
ENPL_HUMAN	11	11	523.79	7.8	2.9	5423087.67	1811483.41
THIO_HUMAN	2	2	125.31	1.7	0.5	5265516.47	1848388.07
ADHX_HUMAN	6	6	405.7	6.2	1.5	5251161.15	1475543.35
PPLA_HUMAN	2	2	71.94	1.7	0.8	5198023.78	2217525.12
1433G_HUMAN	6	2	404.11	2.2	0.8	5185233.99	1308335.89
CAD13_HUMAN	7	7	612.39	7.0	2.0	5088895.08	2772116.19
GLYG_HUMAN	7	7	398.48	4.5	1.0	5073030.18	1105012.15
SUCB2_HUMAN	8	8	507.92	5.2	1.2	5039729.94	2565937.09
CRYM_HUMAN	7	7	368.42	5.0	0.9	5016270.45	1201551.56
CD36_HUMAN	6	6	478.01	5.2	0.8	4967776.49	1890435.84
NACAM_HUMAN	20	18	1105.15	11.2	6.6	4925323.85	4300355.24
K22E_HUMAN	5	3	270.86	0.8	1.3	4908309.44	729793.85
NDUB4_HUMAN	4	4	314.7	4.2	1.0	4861908.93	2841140.86
PROF1_HUMAN	4	4	255.85	4.2	1.3	4744948.50	609922.98
TPP1_HUMAN	3	3	251.74	2.8	0.8	4705501.60	694596.57
GLRX1_HUMAN	3	3	198.86	3.3	0.8	4698821.23	1804363.82
BASI_HUMAN	6	6	381.82	5.5	1.5	4611953.04	884440.05
ADH1B_HUMAN	7	7	336	4.8	1.5	4604245.82	2119067.91
IDH3A_HUMAN	5	5	329.99	4.7	1.0	4509066.42	1376216.76
UGPA_HUMAN	8	8	534.15	6.7	0.5	4470139.40	1202064.33
AOFA_HUMAN	11	7	640.73	7.0	1.5	4447283.79	537630.62
AOFB_HUMAN	9	6	572.46	5.0	0.9	4418626.19	759605.85
DPYL2_HUMAN	11	11	528.42	6.2	1.5	4418505.59	1429738.23
S10A8_HUMAN	4	4	283.62	3.7	1.8	4395707.93	3059666.96
GSTP1_HUMAN	2	2	82.98	1.7	0.5	4325913.31	933213.16
DHPR_HUMAN	6	6	517.22	5.3	1.4	4304415.34	773313.49
LUM_HUMAN	6	6	264.14	4.8	0.8	4287966.67	1329857.15
GLO2_HUMAN	6	6	426.51	5.5	1.2	4255997.40	762464.83
HSPB7_HUMAN	3	3	276.71	2.8	1.0	4246363.01	851454.94
CACP_HUMAN	8	8	381.36	4.8	1.2	4173879.66	841608.84
NDUAC_HUMAN	6	6	357.92	4.7	0.8	4163068.58	1480801.72
MYL6_HUMAN	6	5	359.27	3.8	1.2	4159834.59	922736.94
PDLI1_HUMAN	7	7	490.1	5.3	0.8	4149027.24	931970.07
A2MG_HUMAN	14	14	816.32	8.3	4.6	4127055.38	2521293.21
SMYD1_HUMAN	9	9	567.43	6.8	2.9	4006422.35	935967.82
TACO1_HUMAN	3	3	167.73	1.5	1.0	3906773.36	1069076.33
LAMB1_HUMAN	12	11	721.18	7.0	2.2	3891409.98	1227952.82
RAN_HUMAN	3	3	197.23	2.0	0.9	3881487.98	4158904.70
ITB1_HUMAN	10	10	541.4	7.0	2.0	3874806.50	1175351.25
AT1A3_HUMAN	17	6	1240.33	5.0	1.4	3828119.57	894582.94
HBD_HUMAN	10	4	925.42	2.7	1.9	3744322.84	3830494.60

APOA1_HUMAN	11	11	633.85	4.8	6.7	3686916.88	4476713.29
ES1_HUMAN	3	3	264.54	3.8	1.7	3682758.43	3011033.22
NDUB1_HUMAN	2	2	70.87	1.5	0.5	3677505.34	1715193.85
MOES_HUMAN	14	9	848.81	7.3	1.2	3633386.20	289977.99
ODPX_HUMAN	6	6	306.9	4.8	1.9	3591193.21	1188737.33
MCCB_HUMAN	10	10	778.28	7.3	3.6	3588437.20	1843459.41
QOR_HUMAN	6	6	437.39	5.3	1.2	3528145.24	1113438.68
PCCA_HUMAN	10	10	579.93	7.2	1.2	3506728.92	536780.23
PLAK_HUMAN	11	9	705.06	7.3	2.1	3501068.82	402344.47
ECI2_HUMAN	7	7	611.01	7.0	1.4	3430522.76	1114719.19
PLIN4_HUMAN	13	13	885.5	7.3	4.6	3389545.27	1976966.46
H2B1B_HUMAN	3	2	145.55	1.5	0.5	3382813.30	2183397.89
PGS2_HUMAN	3	3	152.96	2.0	0.6	3352924.88	973460.95
VTDB_HUMAN	5	5	294.05	3.2	1.3	3347726.13	1216955.40
TMOD1_HUMAN	7	7	481.56	6.5	2.1	3344025.11	1353100.89
GDIR1_HUMAN	3	3	185.03	2.3	0.8	3341530.33	410291.43
CN159_HUMAN	10	10	708.68	6.5	6.6	3285643.77	3824516.92
EFTU_HUMAN	8	7	419.24	5.2	1.5	3280605.28	1062973.90
THTR_HUMAN	4	4	297.93	3.3	0.5	3276421.93	1048691.33
ESTD_HUMAN	5	5	394.83	5.0	1.3	3267922.61	959464.81
ANX11_HUMAN	9	8	400.41	6.3	1.2	3252028.96	360357.58
AL9A1_HUMAN	7	7	427.32	5.0	1.1	3205292.65	97854.23
PCCB_HUMAN	10	10	629.96	7.7	1.2	3202452.37	875208.28
CPT2_HUMAN	10	9	530.1	6.5	1.2	3151786.20	410737.74
BDH_HUMAN	8	8	349.03	5.0	2.4	3125786.82	1724143.10
KAD4_HUMAN	4	4	245.13	4.7	0.5	3079244.59	957876.07
ACS2L_HUMAN	8	7	430.66	5.2	1.2	3077098.88	1611056.50
IVD_HUMAN	4	4	261.78	3.2	0.8	3065359.13	529624.88
SAMP_HUMAN	5	5	304.93	3.7	0.5	3059260.20	525013.96
NID2_HUMAN	11	11	801.19	9.0	1.4	3050724.11	226706.80
MCCA_HUMAN	6	6	324.25	3.8	1.6	3039027.09	1803284.71
QCR6_HUMAN	2	2	162.24	2.0	1.1	3035505.35	687697.25
CX7A2_HUMAN	3	3	191.54	2.2	1.2	3021825.68	1014773.61
GDE_HUMAN	12	11	654.09	7.7	2.0	3011970.53	1215071.14
NDKB_HUMAN	3	3	288.87	2.5	1.0	2956364.89	1121091.83
FKB1A_HUMAN	2	2	164.67	1.0	0.6	2948692.79	1272685.65
LEG3_HUMAN	6	6	378.33	4.7	1.9	2942813.21	774464.75
SSDH_HUMAN	6	6	336.36	3.8	0.8	2940556.00	1315243.88
NDUB8_HUMAN	6	6	304.03	4.5	1.9	2904925.00	767049.39
CADH2_HUMAN	5	5	394.83	4.7	1.0	2903976.31	1032439.70
MPC2_HUMAN	4	4	234.72	4.0	1.3	2898922.43	1280102.11
MAP4_HUMAN	13	13	662.76	7.5	4.2	2888552.42	1797816.37
NDUS8_HUMAN	3	3	125.88	2.5	0.8	2884109.58	989266.03
AACT_HUMAN	6	6	281.78	2.8	2.1	2877309.70	1381185.16
PKP2_HUMAN	9	9	513.47	6.2	2.3	2872489.03	503263.03
CD59_HUMAN	3	3	204.22	2.3	1.0	2856537.00	1660997.38
ACOC_HUMAN	9	9	450.84	6.0	3.1	2809749.85	774230.40
ANKR2_HUMAN	9	9	613.7	7.0	2.2	2796871.34	1953039.97
MIF_HUMAN	2	2	100.94	1.7	0.5	2777878.38	1362915.48
AFG32_HUMAN	12	11	486.6	7.0	2.0	2775634.27	1083068.00
SBP1_HUMAN	9	9	478.81	5.8	0.8	2767676.80	338749.20
M2OM_HUMAN	8	8	435.07	5.3	0.8	2763019.42	877231.34
RYR2_HUMAN	17	16	926.64	10.3	2.3	2761667.85	780609.73
NDUA6_HUMAN	4	4	209.14	2.8	0.8	2740138.43	958141.39
SDPR_HUMAN	5	5	369.93	3.8	1.2	2720364.21	260047.54
NID1_HUMAN	10	10	544.57	7.0	2.0	2682362.05	366997.42
IMPA1_HUMAN	4	4	271.41	3.5	1.4	2664806.96	398586.42
DCXR_HUMAN	3	3	225.47	3.2	1.2	2620535.88	815663.24
ACO13_HUMAN	2	2	126.42	1.7	0.5	2617277.85	1346086.03

WDR1_HUMAN	7	7	461.54	6.3	0.8	2543690.78	354139.50
CLH1_HUMAN	10	10	568.24	8.0	2.2	2518300.81	292720.35
PDIA6_HUMAN	6	6	377.32	4.5	1.0	2492711.70	655932.46
PSA6_HUMAN	6	6	424.22	4.7	1.0	2452903.44	832484.27
BAG3_HUMAN	8	8	430.32	5.0	2.2	2444920.97	1029177.36
GYS1_HUMAN	7	7	327.33	4.5	2.1	2439493.01	629780.46
CO4A1_HUMAN	4	3	305.99	2.5	1.0	2417950.22	625184.10
SAM50_HUMAN	6	5	381.23	4.3	1.0	2416632.82	801195.66
DCMC_HUMAN	8	8	571.43	6.3	2.1	2399541.82	769145.19
K1C10_HUMAN	9	9	650.36	5.5	2.4	2381749.35	2164058.96
CX7A1_HUMAN	2	2	131.16	1.7	0.5	2357059.47	402495.13
TAGL_HUMAN	4	4	192.5	3.0	0.9	2354564.19	700744.61
MTCH2_HUMAN	5	5	291.87	4.5	1.0	2348357.18	597547.47
AL7A1_HUMAN	8	8	530.21	5.3	1.2	2345468.52	468629.64
BCAT2_HUMAN	7	7	402.19	3.5	1.5	2276008.60	810485.24
IF5A1_HUMAN	4	4	267.82	5.0	1.3	2267340.87	701270.89
ANXA1_HUMAN	7	7	503.04	5.0	1.8	2242900.38	437055.75
MAOM_HUMAN	7	7	416.74	4.7	1.2	2212313.64	562777.64
OPA1_HUMAN	14	14	665.11	8.2	1.3	2200538.14	710197.85
NDUA8_HUMAN	4	4	198.7	3.2	0.8	2200306.36	533323.59
CO4A2_HUMAN	4	4	210.36	2.5	1.2	2167794.74	222766.30
TLN2_HUMAN	23	19	1286.95	12.8	2.2	2163494.97	431531.30
ARHL1_HUMAN	6	6	229.63	2.8	1.5	2148598.11	1380212.84
TLN1_HUMAN	18	14	1337.56	11.2	2.2	2135576.87	406184.62
CAH1_HUMAN	5	5	248.8	3.3	2.7	2130135.44	1399193.30
NDUS4_HUMAN	2	2	168.85	2.5	0.5	2111635.34	1320626.78
GSTK1_HUMAN	4	4	266.43	2.8	1.6	2092403.94	1224862.51
IDH3B_HUMAN	3	3	315.5	3.2	1.0	2083929.49	1292557.65
DOPD_HUMAN	4	4	214.49	3.0	0.6	2037836.48	1181327.02
LPPRC_HUMAN	17	15	803.18	9.7	1.9	2029835.35	774989.55
NDUAB_HUMAN	3	3	222.3	2.7	0.5	2012317.97	997516.42
AT1A1_HUMAN	18	9	1276.78	5.2	2.3	2002667.69	568164.55
2AAA_HUMAN	6	6	276.54	4.3	1.5	1985530.95	982472.45
DYHC1_HUMAN	18	18	870.26	11.8	0.8	1965874.49	325371.95
HCD2_HUMAN	5	5	330.8	3.3	2.0	1938856.20	871584.71
OBSCN_HUMAN	19	18	979.77	9.8	3.8	1936158.91	557721.27
VTNC_HUMAN	4	4	201.21	2.7	1.0	1934243.44	118009.28
PSA5_HUMAN	4	4	263.3	3.2	1.2	1930003.17	664098.24
CTNB1_HUMAN	6	4	372.24	2.2	1.2	1900265.43	364258.30
CFAB_HUMAN	6	6	330.37	2.7	1.9	1898422.80	824829.66
CTNA1_HUMAN	10	10	591.23	6.5	1.6	1883655.59	386922.45
H2B1L_HUMAN	3	2	148.24	1.7	0.5	1873007.17	784221.26
ABLM1_HUMAN	10	10	551.73	5.8	1.6	1866041.47	424914.44
ODB2_HUMAN	6	6	357.2	3.7	3.1	1858275.21	1325956.50
DYL2_HUMAN	3	3	253.93	3.3	0.5	1855693.56	284768.29
SAHH_HUMAN	8	8	332.45	5.8	1.6	1855012.51	631588.95
GSTM3_HUMAN	7	6	514.2	5.5	1.0	1829848.09	286847.38
SRBS1_HUMAN	15	13	709.55	8.7	1.6	1807556.65	138364.75
RS3_HUMAN	5	5	202.58	3.7	0.5	1804218.10	327171.00
PACN3_HUMAN	7	7	477.54	4.5	1.0	1782983.03	554671.78
TBB4B_HUMAN	14	2	1061.36	2.2	0.8	1771782.50	745823.63
FINC_HUMAN	5	5	225.43	2.7	1.4	1771214.53	146495.99
AUHM_HUMAN	6	6	318.2	4.3	0.5	1762507.71	857381.06
PYGM_HUMAN	11	6	515.2	4.3	0.5	1757176.36	336655.47
ATP5E_HUMAN	2	2	75.79	1.5	0.5	1747273.09	1211638.72
DAG1_HUMAN	5	5	247.74	3.5	1.2	1718455.46	499596.54
UBA1_HUMAN	7	7	531.62	5.8	1.2	1709924.96	448285.11
HEBP2_HUMAN	3	3	154.09	2.0	0.9	1697399.15	557855.11
VAT1_HUMAN	4	4	226.92	2.2	1.2	1682954.32	1357001.46

PIMT_HUMAN	2	2	227.48	2.8	0.4	1676043.59	513383.09
APOH_HUMAN	4	4	220.95	3.3	1.0	1670083.77	388514.95
F10A5_HUMAN	4	4	214.3	2.5	0.5	1660326.88	344047.34
ANXA3_HUMAN	6	6	353.13	4.8	1.2	1656549.43	419174.39
GPX3_HUMAN	3	3	196.21	2.5	1.0	1633513.45	817758.61
ODBA_HUMAN	5	5	226.46	3.3	2.3	1628574.28	852784.40
IPYR2_HUMAN	5	5	308.26	3.7	0.5	1621838.24	571140.88
GLU2B_HUMAN	7	7	393.28	4.7	1.4	1603032.83	229566.79
MIC27_HUMAN	4	4	213.96	3.0	1.4	1600997.41	730479.96
ATPK_HUMAN	3	3	178.55	2.3	1.4	1596730.27	840931.81
GRHPR_HUMAN	5	5	397.17	4.7	1.0	1593778.23	264251.34
ACTG_HUMAN	20	3	1519.04	1.3	1.0	1589881.10	190591.56
F162A_HUMAN	4	4	229.55	2.7	2.1	1583046.86	1035557.36
DYSF_HUMAN	11	11	692.17	7.2	1.5	1568487.30	402047.60
ACDSB_HUMAN	6	6	329.38	4.5	0.5	1563774.82	590364.96
CAPZB_HUMAN	3	3	165.81	2.8	1.2	1557305.07	426874.22
NCAM1_HUMAN	4	4	203.71	2.2	1.2	1543889.17	316925.18
SGCD_HUMAN	2	2	96.26	1.7	0.8	1537089.62	375023.86
MACD1_HUMAN	2	2	154.48	0.8	0.8	1531660.86	492237.86
PP1B_HUMAN	4	4	289.83	3.0	0.6	1530709.62	421113.52
CERU_HUMAN	7	7	458.33	4.5	2.3	1521838.87	1292235.09
TBA4A_HUMAN	10	2	607.89	1.5	0.5	1503198.32	325806.45
PSME1_HUMAN	5	5	296.57	4.2	1.2	1496027.89	683342.77
S10AA_HUMAN	2	2	76.68	1.5	0.5	1484168.92	299682.23
S10A9_HUMAN	2	2	219.41	2.0	1.7	1464645.26	995709.69
ITA7_HUMAN	5	5	237.55	2.5	1.0	1455495.78	168702.03
NPS3B_HUMAN	5	4	277.92	2.8	0.8	1430703.91	453711.32
K2C1_HUMAN	11	7	688.53	3.2	2.3	1424585.76	1083178.64
SSBP_HUMAN	2	2	127.67	1.7	0.5	1424391.00	593808.97
RLA2_HUMAN	4	4	238.94	2.8	1.0	1423055.31	319809.92
PCYOX_HUMAN	6	6	293.43	3.8	2.1	1421859.09	573323.22
1433T_HUMAN	7	3	446.45	3.0	1.1	1393617.55	659503.76
TAGL2_HUMAN	5	5	258.4	4.0	1.1	1375898.85	147653.60
L2HDH_HUMAN	5	5	242.76	3.7	1.8	1374223.01	293540.03
PPIB_HUMAN	4	4	212.37	3.3	0.8	1367226.34	357787.01
ICAL_HUMAN	8	8	440.12	3.5	3.1	1362787.48	1310303.57
PSA_HUMAN	10	10	563.16	7.0	1.5	1360776.93	330504.47
TCPQ_HUMAN	8	8	447.64	4.8	1.6	1358087.41	319864.33
EHD2_HUMAN	7	6	315.53	4.5	1.5	1344535.85	324161.27
GBLP_HUMAN	5	5	285.3	2.8	0.8	1326530.57	364016.22
AT1A2_HUMAN	15	5	1083.8	3.2	1.7	1316089.68	384631.79
PP2AA_HUMAN	5	4	307.17	3.8	1.3	1310879.94	346484.34
LETM1_HUMAN	5	5	292.1	3.8	0.8	1309395.26	525882.29
EHD4_HUMAN	9	8	510.93	4.3	1.6	1308066.36	345517.65
CAH2_HUMAN	3	3	192.96	2.5	1.6	1304851.93	928983.31
CATA_HUMAN	7	7	397.54	3.8	1.5	1280538.92	558362.81
TALDO_HUMAN	3	3	257.94	3.0	1.3	1276265.80	368135.92
MTX2_HUMAN	5	5	256.95	3.5	1.4	1259871.02	136086.53
RL10A_HUMAN	3	3	121.45	2.3	0.5	1258580.27	223088.92
PHP14_HUMAN	2	2	177.13	2.5	0.8	1245544.10	843414.57
FRDA_HUMAN	2	2	147.12	1.7	0.5	1241197.37	286393.94
NIBAN_HUMAN	6	6	358.04	3.2	1.6	1237907.69	576181.66
GSHR_HUMAN	3	3	154.41	2.0	0.9	1223061.73	336216.43
PGS1_HUMAN	4	4	289.26	2.5	1.4	1222801.53	399354.95
ML12A_HUMAN	4	2	251.88	1.7	0.5	1203590.69	345055.49
STIP1_HUMAN	5	5	249.78	2.7	0.5	1203535.27	448148.10
ACOT9_HUMAN	5	5	214.72	3.5	1.4	1201178.17	584683.29
LYPA1_HUMAN	3	3	116.17	1.7	1.0	1196419.61	100968.39
SGCA_HUMAN	4	4	244.83	2.8	1.3	1196025.17	414116.47

RLA0_HUMAN	4	4	321.02	2.8	0.8	1185752.67	287616.09
S10AD_HUMAN	2	2	143	1.8	1.2	1174326.75	387991.88
GDIA_HUMAN	6	5	406.98	4.0	1.1	1158429.96	358541.88
UK114_HUMAN	2	2	122.62	1.2	0.4	1146444.24	340019.71
CNDP2_HUMAN	5	5	259.41	3.2	0.8	1140190.54	217281.77
GSTM2_HUMAN	5	4	333.45	4.0	1.3	1138233.25	356087.39
NEXN_HUMAN	4	4	235.28	2.5	1.2	1136026.41	383621.68
TRXR2_HUMAN	5	4	509.58	3.8	1.0	1119518.25	328250.46
FRIH_HUMAN	6	5	324.58	4.0	0.9	1116293.99	123760.09
GANAB_HUMAN	4	4	223.93	3.2	0.8	1115111.60	122840.10
LMNB2_HUMAN	9	7	370.97	4.0	1.8	1113230.97	188997.80
IDH3G_HUMAN	3	3	145.82	2.0	0.9	1106473.64	324058.15
KAP2_HUMAN	5	4	364.55	2.5	1.4	1104444.97	437872.48
RHOA_HUMAN	3	3	142.56	2.0	1.1	1103645.59	252704.19
SPB6_HUMAN	4	4	237.15	3.2	1.0	1101195.27	317032.82
ACTN4_HUMAN	21	5	1622.87	3.3	1.2	1098979.77	221012.87
EF1G_HUMAN	4	4	212.02	2.3	0.8	1097115.87	193041.34
MECR_HUMAN	3	3	127.28	2.0	0.6	1095449.42	448552.89
RL12_HUMAN	3	3	190.33	2.2	0.8	1078094.57	248894.35
HIBCH_HUMAN	4	4	244.71	2.0	0.9	1077482.18	782015.71
NB5R1_HUMAN	3	3	145.67	1.8	0.8	1073430.86	246920.01
TM143_HUMAN	5	5	223.84	2.5	0.8	1068063.59	262961.83
MSRB2_HUMAN	5	5	210.24	3.7	1.0	1062188.63	309099.61
IDHC_HUMAN	7	6	446.5	5.3	1.8	1056458.00	274526.66
HINT2_HUMAN	2	2	117.23	1.5	0.8	1054515.45	486364.30
LACTB_HUMAN	4	4	183.23	3.5	0.8	1049968.19	475033.44
EZRI_HUMAN	9	4	551.11	2.8	1.0	1045178.41	486149.12
PSA1_HUMAN	5	5	270.96	4.2	1.0	1042645.02	359564.78
AMPL_HUMAN	5	4	274.98	3.0	0.9	1041835.12	62484.74
UB2V1_HUMAN	3	3	117.98	1.8	1.7	1031418.14	229629.67
PNPO_HUMAN	4	4	158.03	2.7	0.8	1027592.83	71374.45
PSB6_HUMAN	3	3	178.73	2.5	1.2	1025581.06	318452.15
ORN_HUMAN	3	3	161.95	2.3	0.5	1025061.54	178324.82
DHB4_HUMAN	4	4	175.94	2.3	1.0	1022154.59	310007.39
GDIB_HUMAN	4	3	229.64	2.2	0.8	1007673.29	315828.04
LG3BP_HUMAN	3	3	190.31	3.2	1.2	1005015.41	264373.38
NTF2_HUMAN	2	2	122.54	1.7	0.5	1003673.32	335822.75
CPNE3_HUMAN	5	5	223.79	3.5	0.8	999967.67	421704.99
SPTB1_HUMAN	13	9	531.59	5.0	1.3	982149.23	156718.08
RS4X_HUMAN	5	5	284.91	3.7	0.5	968387.93	173509.79
RL14_HUMAN	2	2	97.74	1.3	1.2	960667.66	539114.17
TELT_HUMAN	4	4	218.07	2.8	0.8	959286.05	122291.14
SAP_HUMAN	2	2	98.46	1.7	0.5	947281.00	80124.16
NEST_HUMAN	10	10	536.34	5.8	1.2	929790.62	208952.28
CAN2_HUMAN	5	5	252.13	3.2	0.4	925474.46	129708.32
TIM44_HUMAN	5	5	351.23	4.5	0.5	925382.25	213839.82
RS6_HUMAN	4	4	154.33	2.0	1.1	925236.79	231558.93
LONM_HUMAN	7	7	394.41	4.3	2.4	924236.66	366869.62
EF1D_HUMAN	7	4	388.6	3.3	0.5	923059.48	179335.90
RL5_HUMAN	3	3	231.85	2.7	1.2	909884.49	188880.13
SIR5_HUMAN	4	4	201.16	2.3	1.2	902183.12	544656.02
FETUA_HUMAN	2	2	160.02	1.7	0.5	868694.52	394681.04
RS8_HUMAN	5	5	305.73	2.8	1.0	858181.39	235998.33
CO9_HUMAN	2	2	81.88	0.7	1.0	855822.81	480698.72
SYWC_HUMAN	5	5	304.76	3.3	1.2	841975.84	169672.23
SYNEM_HUMAN	6	6	310.62	3.5	0.5	839779.80	198214.47
COF1_HUMAN	3	2	219.11	1.5	0.8	839708.81	356203.67
ACAD8_HUMAN	4	4	227.03	3.2	1.5	832395.84	203378.07
ROA2_HUMAN	3	3	187.05	2.2	0.8	819987.87	278757.65

RS3A_HUMAN	2	2	117.59	1.0	0.6	819351.00	173116.61
CRP_HUMAN	2	2	91.18	1.7	0.5	810281.47	523842.07
MOT1_HUMAN	2	2	133.49	1.7	1.4	801509.15	197942.68
SODC_HUMAN	2	2	166.98	1.8	1.2	800643.70	413375.95
RAB2A_HUMAN	4	4	225.51	3.0	0.6	800445.84	129628.03
HEMH_HUMAN	6	6	318.43	3.5	1.2	799777.55	165638.51
CPNS1_HUMAN	2	2	98.83	1.5	0.5	796403.58	219983.86
HOT_HUMAN	5	5	262.71	3.8	0.8	792490.99	190219.66
FUND2_HUMAN	2	2	136.94	0.7	0.8	792171.46	279304.14
NPS3A_HUMAN	4	3	223.66	2.7	0.8	790574.00	106836.89
RMD1_HUMAN	4	4	189.79	2.7	1.6	787973.16	360481.09
ISOC1_HUMAN	3	3	225.91	2.5	1.0	783636.40	269478.54
HMGB1_HUMAN	3	3	215.23	2.5	1.2	782372.58	238420.04
RL23A_HUMAN	2	2	112.16	1.2	0.8	773790.29	188738.14
TCPG_HUMAN	7	7	323.1	4.0	1.7	773474.34	185056.41
RS16_HUMAN	2	2	132.77	1.7	0.8	771758.52	208388.13
MUTA_HUMAN	4	4	222.81	3.0	2.5	769990.33	466756.21
SGCG_HUMAN	3	3	201.64	2.5	0.5	768166.00	262577.16
NAC1_HUMAN	4	4	195.86	2.8	1.5	766570.61	253473.32
RL7A_HUMAN	3	3	170.22	1.8	0.4	764840.10	250008.08
PSB4_HUMAN	3	3	135.13	1.8	0.8	760826.03	194936.13
MCEE_HUMAN	2	2	71.21	1.3	0.5	750043.23	166225.00
BCS1_HUMAN	4	4	172.99	3.2	0.8	749896.25	235210.89
C1QBP_HUMAN	2	2	157.22	1.8	0.8	743131.70	152482.97
FIBA_HUMAN	2	2	134.93	1.3	0.8	742653.63	612472.74
FERM2_HUMAN	2	2	135.93	1.3	0.8	739946.15	63100.27
EST2_HUMAN	4	4	216.34	4.0	1.4	736404.01	239936.55
COQ7_HUMAN	2	2	120.58	1.7	0.5	734454.64	181522.80
SYP2L_HUMAN	4	4	233.85	1.8	1.3	733077.05	396025.33
HNRDL_HUMAN	3	3	165.83	2.3	1.4	732162.44	235721.20
ELOC_HUMAN	2	2	138.76	1.7	0.5	730667.05	307555.37
UN45B_HUMAN	5	5	234.48	2.7	1.0	727191.27	278708.56
ERP29_HUMAN	4	4	229.52	3.3	0.5	720154.49	182563.88
S10AB_HUMAN	2	2	91.71	0.7	0.5	714116.02	115592.57
SPRE_HUMAN	3	3	175.69	2.3	0.5	712261.50	93972.96
ILK_HUMAN	3	3	120.94	2.3	1.2	711275.99	116699.33
GLOD4_HUMAN	5	5	240.74	3.2	1.2	710231.41	152953.05
RS20_HUMAN	2	2	69.85	1.2	0.4	709052.07	43920.43
PRAF3_HUMAN	2	2	82.63	1.2	0.8	696064.78	145768.42
DUS3_HUMAN	3	3	215.81	1.7	0.8	694960.72	532051.88
CATZ_HUMAN	3	2	139.63	1.0	0.6	693060.87	227181.60
ODBB_HUMAN	2	2	121.89	1.7	0.5	689596.40	309009.55
HSP74_HUMAN	8	7	492.36	4.2	2.0	687114.96	279945.75
SGCB_HUMAN	3	3	188.99	2.0	0.6	683275.98	94730.87
TMM65_HUMAN	2	2	122.39	2.5	1.2	682888.38	149558.65
NQO2_HUMAN	2	2	126.43	1.5	0.5	680437.01	407316.77
NNRE_HUMAN	2	2	120.12	1.8	1.3	679922.98	439909.90
FIS1_HUMAN	2	2	97.01	1.7	0.5	679279.64	331516.71
CLCB_HUMAN	2	2	81.66	1.2	0.8	672135.59	133265.30
A2GL_HUMAN	4	3	179.32	2.2	1.8	667701.72	310166.75
CDC37_HUMAN	3	3	144.2	2.0	1.3	665616.13	131870.35
RS25_HUMAN	2	2	121.74	1.5	0.5	663920.51	203601.74
CALU_HUMAN	2	2	165.23	1.8	0.8	662218.04	178768.95
BCAM_HUMAN	4	4	227.29	2.5	0.8	658420.88	154816.08
RAB7A_HUMAN	3	3	189.34	2.0	0.9	657550.53	134504.93
TIM13_HUMAN	2	2	135.68	1.7	0.5	656085.76	196506.09
KAP0_HUMAN	4	4	239.87	3.7	1.4	655860.70	111271.10
CLIC4_HUMAN	2	2	178.53	1.8	1.3	654213.52	465791.75
MYPT2_HUMAN	4	4	339.31	2.8	1.0	651511.96	187705.16

TXNL1_HUMAN	3	3	142.44	2.3	0.8	647650.30	143615.58
K1C9_HUMAN	6	6	429.12	2.8	2.1	647485.53	542466.24
MCAT_HUMAN	3	3	124.43	2.0	0.9	632903.79	196422.33
RS9_HUMAN	3	3	97.5	2.3	0.5	632577.45	37644.99
RL11_HUMAN	2	2	97.45	1.7	1.0	630663.28	108087.30
PSB1_HUMAN	2	2	86.81	1.2	0.4	629389.41	198729.04
JPH2_HUMAN	5	5	242.39	3.5	1.5	628570.80	271013.39
ABEC2_HUMAN	2	2	77.81	1.5	0.5	627064.72	91592.22
TCPB_HUMAN	3	3	197.88	1.8	0.8	626548.45	353989.33
NFS1_HUMAN	5	5	321.27	3.7	2.0	623384.78	237156.54
TCPA_HUMAN	6	5	259.46	3.7	1.0	611324.33	175181.86
PCBP1_HUMAN	3	2	183.33	1.5	0.5	608876.79	233179.22
68MP_HUMAN	2	2	67.13	1.5	0.5	608454.90	302313.31
LIS1_HUMAN	3	3	215.33	2.3	0.8	604594.08	162198.03
NFU1_HUMAN	3	2	244.7	2.5	0.5	600281.14	230931.19
TRAP1_HUMAN	7	6	435.52	3.0	1.3	598603.43	329493.41
RL15_HUMAN	2	2	107.87	1.0	0.6	598319.86	108781.61
ALAT1_HUMAN	4	4	224.67	2.5	1.0	592720.77	198254.70
SAA1_HUMAN	2	2	132.23	1.8	1.2	591906.24	341123.40
ECHD3_HUMAN	3	3	159.7	1.8	1.0	590968.12	202685.89
HSPB2_HUMAN	2	2	126.21	1.5	0.5	582672.81	237339.98
PSB5_HUMAN	3	3	182.84	1.8	0.8	580187.90	213708.71
SFXN1_HUMAN	3	3	178.27	2.5	0.5	577973.23	156065.09
SUOX_HUMAN	3	3	123.66	2.3	0.8	577649.59	110922.48
RTCB_HUMAN	4	4	174.97	2.3	0.5	576705.90	130301.70
RAC1_HUMAN	2	2	90.93	1.7	0.5	571299.40	87664.32
LGUL_HUMAN	3	3	139.36	2.5	0.5	566323.60	201460.29
HNRPK_HUMAN	3	3	189.25	1.5	1.0	561585.39	231968.03
CAN1_HUMAN	4	4	196.49	2.7	1.0	558201.58	121722.72
HEBP1_HUMAN	3	3	182.58	2.5	0.8	556498.58	102357.94
IGHG3_HUMAN	7	2	393.65	1.7	2.6	548028.89	661712.61
HNRH1_HUMAN	4	4	160.2	2.7	0.8	547837.87	95092.19
LMAN1_HUMAN	4	4	196.43	2.7	1.8	541573.24	327051.88
USO1_HUMAN	4	4	253.37	2.0	1.3	539109.97	159262.58
COFA1_HUMAN	3	3	142.28	2.2	0.8	538570.42	179001.39
CTNA3_HUMAN	6	6	369.57	3.0	2.0	538135.40	197285.80
DDB1_HUMAN	6	6	287.62	4.3	1.0	537709.22	238008.02
COQ5_HUMAN	3	3	136.88	1.8	1.0	537652.75	185396.74
SNAA_HUMAN	5	5	275.88	3.5	1.0	535891.34	95953.16
CLUS_HUMAN	3	3	180.67	1.0	1.3	533187.71	324584.20
ADT2_HUMAN	10	2	481.34	0.7	0.5	532606.54	168396.80
CKAP4_HUMAN	5	4	322.25	3.5	0.8	530789.10	130335.70
TPM4_HUMAN	11	2	761.81	0.8	0.8	523085.47	144860.55
NDUA3_HUMAN	2	2	75.68	1.0	0.0	519601.56	303098.22
NP1L4_HUMAN	3	3	163.62	2.3	0.5	519413.30	184070.74
PDIA4_HUMAN	6	6	318.6	4.3	2.3	518427.19	209357.26
NUCL_HUMAN	2	2	88.82	1.0	0.6	512574.52	224958.09
PNPT1_HUMAN	6	6	307.48	3.3	1.8	511788.30	293473.24
TXND5_HUMAN	4	4	207.78	2.7	0.5	509129.68	125547.70
XRCC6_HUMAN	3	3	171.25	1.5	0.5	507938.39	98249.92
A1BG_HUMAN	3	3	128.12	1.2	1.2	505661.02	372968.75
IMB1_HUMAN	2	2	93.97	1.7	0.5	504726.01	156031.27
SPRY4_HUMAN	2	2	91.25	1.2	0.4	497048.48	345483.13
CBR1_HUMAN	4	4	245.42	3.2	0.8	492307.95	110511.45
PHS2_HUMAN	2	2	91.01	1.2	0.4	491815.70	84282.05
NCEH1_HUMAN	3	3	134.55	2.0	1.4	490276.30	215502.43
RD23B_HUMAN	2	2	71.54	0.5	0.5	489898.52	165100.79
PDC6I_HUMAN	4	4	196.74	2.7	1.0	487635.79	139371.64
TINAL_HUMAN	3	3	172.86	2.2	1.2	483287.22	175106.90

AAMDC_HUMAN	2	2	132.04	1.2	0.8	481873.56	261926.15
THRB_HUMAN	3	3	135.5	1.0	1.5	480516.93	469216.71
PDLI3_HUMAN	3	3	212.43	2.8	0.8	476512.76	151979.87
PSA4_HUMAN	5	5	275.29	3.5	1.2	474311.64	167692.23
HEM2_HUMAN	3	3	141.33	1.8	1.3	471902.60	212127.56
LAMA5_HUMAN	9	9	519.82	3.7	2.9	471458.07	196051.62
PCBP2_HUMAN	4	3	227.61	1.8	1.0	468538.94	176325.50
CYB5_HUMAN	2	2	104.07	1.7	0.5	465145.25	103384.02
MTCH1_HUMAN	5	3	253.98	2.5	0.8	463517.29	129963.91
NIPS1_HUMAN	4	3	166.61	2.0	1.3	461998.07	109937.26
MPPB_HUMAN	5	4	204.55	2.8	0.8	459741.10	134302.39
NRAP_HUMAN	5	5	256.83	2.7	1.9	458808.95	103105.15
MYO1C_HUMAN	5	5	225.88	2.3	1.2	458025.91	182918.12
PPAC_HUMAN	2	2	127.85	1.0	0.6	455890.49	100321.88
CA2D1_HUMAN	6	6	263.48	3.3	1.4	455394.30	146811.97
1433F_HUMAN	6	3	409.2	2.2	1.0	454155.31	82545.65
RL8_HUMAN	2	2	107.58	1.3	0.8	448862.31	208843.95
OLA1_HUMAN	2	2	75.81	1.2	0.8	446215.45	154392.94
PA2G4_HUMAN	3	3	124.51	1.7	1.0	444137.94	95391.08
PFKAP_HUMAN	8	5	369.15	3.5	2.4	443326.77	83543.52
SNTA1_HUMAN	2	2	100.79	1.5	0.5	442361.71	145370.04
UBC12_HUMAN	3	3	128.01	1.7	0.8	438820.13	95989.24
PRS7_HUMAN	4	4	246.08	2.2	0.8	438666.13	138367.57
BST2_HUMAN	2	2	101.43	1.2	1.0	438099.00	249122.87
HYOU1_HUMAN	2	2	127.01	1.7	0.5	437921.88	139388.78
CCD58_HUMAN	3	3	144.61	1.5	0.5	437368.15	127002.13
IPYR_HUMAN	3	3	216.88	2.2	0.8	437353.90	68066.19
SYNP2_HUMAN	4	4	223.68	2.0	0.6	436367.38	251758.51
CO4B_HUMAN	6	6	236.61	2.5	2.1	436238.95	409276.46
NAMPT_HUMAN	3	3	171.65	2.2	1.2	434295.67	145249.05
ARK72_HUMAN	3	3	152.51	1.8	0.8	428779.34	19118.13
SCPDL_HUMAN	3	2	152.47	1.7	0.5	426482.65	249661.22
NIT2_HUMAN	6	6	347.58	4.0	1.8	421584.92	106274.76
TFAM_HUMAN	3	3	145.62	2.5	0.8	418627.93	143903.89
RL18_HUMAN	3	3	202.33	2.0	0.6	417606.21	125686.05
PGES2_HUMAN	2	2	134.01	1.7	0.5	417045.29	57103.98
RAB1B_HUMAN	4	2	192.44	1.2	0.4	416245.63	76183.99
H10_HUMAN	2	2	97.06	1.3	0.5	402019.68	166647.97
RM12_HUMAN	2	2	109.49	1.5	0.5	400792.99	159367.90
MAOX_HUMAN	2	2	66.27	1.3	0.8	400672.66	167341.26
MIC26_HUMAN	2	2	109.87	1.5	0.5	393660.07	248808.14
LKHA4_HUMAN	4	4	280.3	2.5	1.6	391505.13	188936.01
PABP4_HUMAN	3	3	158.58	1.8	0.8	391490.60	136397.69
TCTP_HUMAN	2	2	82.77	1.0	0.6	390362.27	140735.62
DNJA3_HUMAN	2	2	122.83	1.7	0.5	390108.18	91282.89
RL6_HUMAN	2	2	104.27	1.7	0.5	388406.75	48113.65
MGST3_HUMAN	2	2	113.36	1.3	1.0	385812.38	158560.16
B2MG_HUMAN	2	2	73.86	1.3	0.5	380747.47	155739.29
AL1A1_HUMAN	6	3	254.58	1.5	0.5	378740.93	18761.88
TCPD_HUMAN	2	2	77.52	1.0	0.6	372069.64	111234.88
DTNB_HUMAN	2	2	102.33	1.7	0.5	370538.01	150939.52
AK1A1_HUMAN	5	4	238.39	3.3	1.2	368987.12	117879.75
PSMD2_HUMAN	3	3	184.36	2.5	1.0	364138.52	70657.62
FA9_HUMAN	4	4	210.4	1.5	1.6	362390.51	398571.48
DDX1_HUMAN	4	4	204.01	2.2	1.8	361896.59	115117.30
SNX3_HUMAN	2	2	76.79	1.3	0.5	361889.24	307628.05
CALD1_HUMAN	4	4	245.8	2.0	1.7	358335.81	167206.34
RL3L_HUMAN	3	3	175.11	2.2	0.8	358169.52	79518.53
OST48_HUMAN	2	2	94.43	1.5	0.5	356986.87	128140.71

C1TC_HUMAN	4	4	203.52	2.7	1.2	354574.27	176131.95
CO8A_HUMAN	2	2	80.97	0.8	1.0	352534.34	350980.41
PDPR_HUMAN	2	2	82.61	1.2	1.0	345951.08	104875.08
EMAL2_HUMAN	2	2	126.27	1.2	1.0	342265.24	150099.80
COA6_HUMAN	2	2	106.5	1.7	1.0	339906.26	248128.10
GLRX5_HUMAN	3	3	156.32	1.5	1.0	337103.60	176403.61
KCY_HUMAN	4	4	205.07	2.2	1.2	335626.33	198354.06
PTGDS_HUMAN	2	2	167.52	1.7	0.5	334617.78	128203.07
GRPE1_HUMAN	3	3	158.37	1.7	0.8	334261.70	176100.56
RPN1_HUMAN	3	3	145.83	2.5	0.5	331741.69	145694.46
SYIM_HUMAN	4	3	250.76	1.5	0.5	331515.54	130295.86
HNRPQ_HUMAN	2	2	89.88	1.3	0.5	330541.47	98953.28
PRELP_HUMAN	3	3	114.11	1.5	0.5	322557.37	173190.04
GLGB_HUMAN	4	4	218.49	3.0	0.9	322462.69	116036.23
RL13_HUMAN	3	3	124.14	1.2	1.0	322016.26	139217.24
PREP_HUMAN	2	2	98.68	1.2	0.8	321934.00	174561.56
RAP1B_HUMAN	2	2	85.09	1.0	0.6	318384.85	104888.48
ENOG_HUMAN	4	2	234.2	1.5	0.8	316721.42	80575.62
F136A_HUMAN	2	2	88.23	0.5	0.8	315804.36	50544.30
ARP3_HUMAN	2	2	95.47	1.7	0.5	314535.71	107619.14
CAP2_HUMAN	3	3	144.38	1.8	0.8	311969.80	98495.46
TATD1_HUMAN	3	3	157.55	1.3	0.8	311517.97	57095.80
RET4_HUMAN	3	3	124.41	1.5	1.2	309897.79	356567.01
PALLD_HUMAN	3	2	185.06	1.3	0.8	308282.08	75516.83
MFN2_HUMAN	4	4	196.37	2.7	0.8	306992.41	32736.70
ITIH2_HUMAN	3	3	217.59	1.3	1.0	306863.45	300368.35
GSHB_HUMAN	3	3	142.33	1.7	1.0	305492.21	136326.72
6PGD_HUMAN	2	2	115.68	1.2	1.0	305384.44	107979.09
CSN4_HUMAN	3	3	159.17	0.8	1.2	302566.54	114360.31
KTN1_HUMAN	4	4	248.95	3.2	1.0	300930.92	100180.38
DCTN1_HUMAN	3	3	209.61	1.2	1.0	298604.09	34766.32
ANT3_HUMAN	2	2	110.07	1.3	0.5	297029.65	240586.50
LYPL1_HUMAN	2	2	75.65	1.2	1.0	296302.53	150791.82
VPS35_HUMAN	3	3	160.36	1.5	1.0	296042.47	88454.42
RS19_HUMAN	2	2	126.85	1.7	0.5	288317.31	71922.26
EST1_HUMAN	2	2	89.56	1.3	0.5	283085.01	94268.93
TCPE_HUMAN	3	3	121.15	1.3	1.2	276948.47	136546.34
PGRC2_HUMAN	2	2	138.25	1.5	0.8	275978.97	101112.37
SIAS_HUMAN	3	3	130.56	1.0	1.1	274629.21	103053.56
SODE_HUMAN	3	3	164.93	2.2	1.0	273634.04	19317.47
GPX1_HUMAN	2	2	109.34	1.7	0.5	269505.97	94161.90
MFAP5_HUMAN	2	2	104.95	1.5	0.8	268758.89	194633.12
MYH14_HUMAN	7	5	419.34	1.3	1.5	268176.72	37995.99
MARC2_HUMAN	3	3	160.49	2.3	0.8	267506.13	51774.32
SFPQ_HUMAN	3	3	129.01	1.2	0.8	266140.33	82981.62
CLIC1_HUMAN	2	2	98.68	1.5	0.5	263190.89	107701.93
ROA1_HUMAN	2	2	91.5	1.2	0.4	260002.63	25987.24
RL4_HUMAN	2	2	99.12	1.5	0.5	257719.29	83100.78
BGH3_HUMAN	2	2	88.96	1.7	0.5	257674.90	78448.19
MPPA_HUMAN	2	2	82.69	1.3	0.8	254332.87	44323.46
IC1_HUMAN	2	2	131.5	1.2	1.5	252480.90	286092.36
TMLH_HUMAN	3	3	130.33	2.2	0.8	252292.81	67485.28
AT2B4_HUMAN	2	2	143.61	1.2	0.4	250222.88	77121.45
FLNB_HUMAN	8	4	407.73	1.7	0.8	247851.56	48197.12
ANXA4_HUMAN	2	2	113.8	1.7	0.8	247666.72	16776.11
TIM9_HUMAN	2	2	108.24	1.0	0.9	245486.53	202715.54
PTGR1_HUMAN	2	2	156.54	1.3	1.0	242988.53	165956.20
ILEU_HUMAN	2	2	105.35	0.5	0.5	242487.78	128291.22
MARCS_HUMAN	3	3	185.15	1.0	1.3	241248.95	215477.33

CK054_HUMAN	2	2	94.86	1.2	1.0	239601.27	80285.87
HNRPM_HUMAN	4	4	201.69	2.7	1.0	239054.40	22316.17
PSMD6_HUMAN	2	2	116.9	1.5	0.8	238771.07	116446.48
RS13_HUMAN	2	2	93.45	1.7	0.8	238197.20	58053.86
ACAD9_HUMAN	2	2	76.52	1.2	0.8	235832.22	79070.25
RL7_HUMAN	2	2	78.72	1.2	0.4	233787.81	42190.91
RAB18_HUMAN	2	2	95.42	1.5	0.5	233678.48	92657.15
NSF1C_HUMAN	3	3	231.13	2.2	1.0	232104.27	108227.50
COQ6_HUMAN	3	3	127.71	1.8	1.0	230392.69	85327.41
MVP_HUMAN	2	2	111.39	1.3	0.5	229339.02	52166.58
PRPS1_HUMAN	3	3	159.23	2.2	0.8	225778.03	50339.97
DNJB6_HUMAN	4	4	268.32	3.7	0.8	223394.60	88027.89
GPDA_HUMAN	2	2	123.72	1.3	0.5	222955.93	49357.07
TENS1_HUMAN	3	3	205.42	1.5	0.5	220555.05	83285.87
MUC18_HUMAN	2	2	74.36	1.5	0.8	218602.34	60202.61
FBLN5_HUMAN	3	3	179.23	1.7	0.8	218338.87	125834.22
SQRD_HUMAN	4	4	167.84	2.0	1.7	218087.11	100569.88
KCD12_HUMAN	3	3	145.28	2.2	0.8	216247.87	48671.27
VAPB_HUMAN	4	2	230.03	1.0	0.6	209970.58	34848.87
PDXK_HUMAN	2	2	78.06	0.8	0.8	208335.19	123528.90
NDUF4_HUMAN	2	2	86.21	1.7	0.5	200975.58	90693.12
PFD2_HUMAN	2	2	93.01	1.5	0.8	199724.94	83258.40
MAON_HUMAN	2	2	83.14	0.5	0.5	197965.83	33032.58
STRAP_HUMAN	3	3	132.98	2.0	0.0	197784.89	34008.57
ITIH1_HUMAN	2	2	93.82	1.3	0.5	196630.86	134086.98
SGTA_HUMAN	2	2	115.76	1.2	0.8	195059.24	104370.42
HNRPU_HUMAN	2	2	96.05	1.5	0.5	193076.34	19371.39
PLSL_HUMAN	3	2	168.35	1.0	0.9	191894.52	154398.20
SYK_HUMAN	2	2	86.39	0.8	0.4	191528.62	49197.82
ZADH2_HUMAN	2	2	115.56	1.2	0.8	190260.37	80696.50
C163A_HUMAN	3	3	164.8	1.3	1.0	189113.48	77087.84
AOC3_HUMAN	2	2	72.89	1.3	0.8	187685.89	68348.15
UFD1_HUMAN	3	3	167.56	1.5	1.2	186556.14	92811.45
RAB5B_HUMAN	2	2	79.63	0.7	0.8	184933.42	31937.90
RL30_HUMAN	2	2	121.06	1.7	0.8	183995.52	92183.00
DNM1L_HUMAN	3	3	138.32	1.5	0.8	183264.30	94710.90
RHG01_HUMAN	2	2	106.6	1.0	0.6	182145.55	27191.97
UBP14_HUMAN	2	2	124.75	1.3	1.0	180700.94	103222.46
LBP_HUMAN	2	2	84.86	1.5	0.5	179666.28	87061.12
DSG2_HUMAN	2	2	113.93	1.3	0.5	178859.31	113095.23
XPP1_HUMAN	3	2	158.44	1.0	0.6	177926.97	67895.23
CC141_HUMAN	2	2	65.1	1.2	0.8	173274.83	67729.43
STOM_HUMAN	2	2	78.23	0.8	0.4	170578.01	39268.70
ETHE1_HUMAN	2	2	112.26	1.2	0.4	170402.31	130775.26
ATPF1_HUMAN	2	2	108.3	1.7	0.5	168175.58	27776.58
RT23_HUMAN	2	2	86.79	1.3	0.8	167187.52	53654.04
LMOD2_HUMAN	2	2	102.54	1.2	0.8	165829.48	61616.06
RS10_HUMAN	2	2	93.01	0.7	1.0	165593.60	89522.16
TCPH_HUMAN	2	2	122.19	1.7	0.5	164954.89	68771.30
PDK4_HUMAN	2	2	90.33	0.8	1.0	163635.79	206464.90
ARF1_HUMAN	4	2	173.06	1.3	0.8	159691.90	37753.92
SYEP_HUMAN	4	4	197.86	1.8	1.3	159456.89	92695.88
MLEC_HUMAN	2	2	107.18	1.5	1.2	159325.90	58152.40
SMD3_HUMAN	2	2	107.91	1.2	0.4	158991.24	51112.83
STML2_HUMAN	3	3	167.46	2.3	0.5	157746.35	42548.99
RS12_HUMAN	2	2	88.02	1.2	0.8	156826.21	40314.30
PDCD5_HUMAN	2	2	105.14	0.8	0.4	155287.46	98226.18
MYPN_HUMAN	3	2	142.13	1.7	0.5	154569.15	52748.27
CBX3_HUMAN	2	2	86.21	0.8	0.4	154379.00	66766.31

COX20_HUMAN	2	2	94.6	1.2	0.4	151526.82	118605.77
DLRB1_HUMAN	2	2	132.16	1.0	0.6	151524.97	42251.85
LMO7_HUMAN	3	3	101.71	1.3	0.8	149502.43	61972.67
IQGA1_HUMAN	2	2	107.33	1.5	0.5	148958.43	37712.81
PPT1_HUMAN	2	2	163.19	1.7	0.5	147587.36	81126.22
PSMD9_HUMAN	3	3	123.41	1.5	0.8	144682.65	26752.49
TOM70_HUMAN	2	2	94.06	1.2	1.0	143591.45	102565.83
XRCC5_HUMAN	2	2	87.75	1.7	0.8	143093.76	20626.16
CFAH_HUMAN	2	2	73.25	1.2	0.8	142208.93	57382.27
BAG2_HUMAN	2	2	169.06	1.3	1.0	140837.50	37152.58
DNJB4_HUMAN	2	2	108.97	1.3	1.0	140176.95	40360.53
TSP4_HUMAN	2	2	73.71	0.7	0.8	138214.43	74948.68
AMPB_HUMAN	2	2	92.6	1.0	0.9	137983.42	19375.31
MYLK3_HUMAN	2	2	146.86	1.3	0.5	137963.88	141655.94
PPCE_HUMAN	2	2	100.09	0.7	0.5	137617.28	46226.02
SCRB2_HUMAN	3	2	162.79	1.7	0.5	131661.55	24568.97
TNNI1_HUMAN	2	2	75.56	0.7	0.8	131377.52	148050.24
CAH3_HUMAN	2	2	99.68	1.5	1.2	130168.34	124061.80
NLRX1_HUMAN	3	3	139.71	1.2	1.2	128042.88	105051.72
APOB_HUMAN	3	3	136.44	0.7	1.2	124989.00	183739.01
TFR1_HUMAN	2	2	115.01	1.0	0.9	124829.05	53433.16
CHCH7_HUMAN	2	2	89.68	1.7	1.0	124683.72	19412.00
CREL1_HUMAN	2	2	92.26	0.7	1.0	122724.23	35249.22
SEPT7_HUMAN	3	2	116.89	0.7	0.8	121801.07	48643.57
PLMN_HUMAN	2	2	83.26	1.0	0.9	120979.17	128449.95
CMBL_HUMAN	2	2	92.21	1.7	0.5	119769.99	50856.43
BAP29_HUMAN	2	2	84.87	1.7	0.5	119407.23	45562.70
HDHD2_HUMAN	2	2	91.6	1.7	0.5	117198.38	20588.87
MAP1B_HUMAN	3	3	130.38	2.2	0.8	113854.32	28076.10
PLIN3_HUMAN	2	2	163.99	0.7	0.8	113234.33	85795.40
PDK1_HUMAN	2	2	108.54	1.2	0.4	110804.01	47113.01
EMIL2_HUMAN	2	2	121.83	1.2	0.8	108932.95	42025.97
CISD2_HUMAN	2	2	129.27	1.2	1.0	106348.55	24621.62
GNPI1_HUMAN	2	2	114.63	1.2	1.0	106253.01	40741.21
UFC1_HUMAN	2	2	75.01	1.2	0.8	105268.30	37449.82
MTX1_HUMAN	2	2	110.13	1.0	0.6	104235.39	74283.75
PLCX3_HUMAN	2	2	78.08	0.8	0.8	102784.49	61209.04
SH3L1_HUMAN	2	2	76.34	1.0	0.6	101226.29	20130.38
PSA7_HUMAN	2	2	121.77	0.8	0.8	100399.72	46387.76
PDCD6_HUMAN	2	2	103.54	0.8	0.4	99922.67	31944.43
PCY2_HUMAN	2	2	74.36	0.3	0.8	97606.82	76780.28
1A69_HUMAN	6	2	335.19	1.0	0.9	96480.77	101807.00
SLIRP_HUMAN	2	2	107.67	0.7	0.5	95204.70	69616.20
HV303_HUMAN	2	2	90.52	1.2	0.8	94740.99	50814.72
ACY1_HUMAN	2	2	71.4	1.0	0.6	92511.42	28292.19
SYNC_HUMAN	2	2	129.52	1.5	0.5	91050.15	31412.47
CSN7A_HUMAN	3	3	183.26	1.3	0.5	90749.94	37371.13
IPO5_HUMAN	2	2	168.14	1.5	0.5	89617.82	39053.47
ARF4_HUMAN	3	2	140.8	1.2	0.8	88849.71	28657.33
TNPO1_HUMAN	2	2	126.27	1.3	0.5	88632.39	46357.19
BZW2_HUMAN	2	2	81.74	1.0	0.9	88333.30	90680.60
RDH13_HUMAN	2	2	69.74	0.5	0.5	88311.47	72191.32
NNRD_HUMAN	2	2	96.77	1.0	0.9	87798.50	14957.58
D2HDH_HUMAN	2	2	94.42	0.8	0.8	83391.45	24024.27
SYNPO_HUMAN	2	2	120.82	1.0	0.6	82268.58	16218.68
MIPEP_HUMAN	2	2	98.15	1.3	1.0	80261.31	55861.95
AL1B1_HUMAN	3	2	125.06	0.8	1.0	78695.64	73629.71
FRIL_HUMAN	2	2	103.09	1.3	1.2	77591.97	32298.41
NAR3_HUMAN	2	2	75.82	1.0	0.9	75424.29	34832.43

SURF1_HUMAN	2	2	76.29	1.3	0.5	74939.36	50223.05
APOD_HUMAN	2	2	133.58	0.8	1.0	74749.55	51242.53
NLTP_HUMAN	2	2	86.08	0.7	0.8	73245.53	60280.92
U2AF2_HUMAN	2	2	84.43	1.5	0.5	72798.14	29525.73
PEDF_HUMAN	2	2	109.62	0.8	1.0	72695.62	57906.42
MAT2B_HUMAN	2	2	80.19	0.7	0.5	71785.95	16434.16
LAMA4_HUMAN	2	2	108.4	1.2	0.8	70414.37	25931.24
ACSF2_HUMAN	2	2	105.13	0.5	0.8	70218.52	49176.79
MLIP_HUMAN	2	2	116.74	0.8	1.0	68075.08	100403.81
STBD1_HUMAN	2	2	115.84	1.3	0.5	67317.75	37869.56
ARC1A_HUMAN	2	2	94.66	1.0	0.6	65396.56	42114.76
CSN6_HUMAN	2	2	74.61	1.2	0.4	62952.92	29997.81
ITIH4_HUMAN	2	2	76.95	1.0	0.9	62122.85	62535.49
PTCD3_HUMAN	2	2	103.08	0.7	1.0	59442.85	41778.92
EP15R_HUMAN	2	2	128.9	1.5	0.5	57798.42	28756.68
TMM43_HUMAN	2	2	74.71	1.7	0.5	56835.45	15613.19
SND1_HUMAN	2	2	66.56	0.5	0.5	55356.29	23471.55
ANK3_HUMAN	3	2	143.33	0.8	0.4	49450.56	13153.34
MYH11_HUMAN	6	2	381.95	1.0	0.6	45154.73	12066.81
TPP2_HUMAN	2	2	87.55	0.8	0.8	43974.06	7734.63
SPG7_HUMAN	2	2	99.4	1.5	0.8	40716.20	16727.90
MIRO1_HUMAN	2	2	87.89	1.2	0.8	39217.60	11696.36
TENX_HUMAN	2	2	80.68	1.2	1.0	36404.00	18999.57

REFERENCES

1. Guyette JP, Gilpin SE, Charest JM, Tapias LF, Ren X, Ott HC. Perfusion decellularization of whole organs. *Nature protocols*. 2014;9:1451-1468
2. Crapo PM, Gilbert TW, Badylak SF. An overview of tissue and whole organ decellularization processes. *Biomaterials*. 2011;32:3233-3243
3. Magrane M, Consortium U. Uniprot knowledgebase: A hub of integrated protein data. *Database : the journal of biological databases and curation*. 2011;2011:bar009
4. Ashburner M, Ball CA, Blake JA, Botstein D, Butler H, Cherry JM, Davis AP, Dolinski K, Dwight SS, Eppig JT, Harris MA, Hill DP, Issel-Tarver L, Kasarskis A, Lewis S, Matese JC, Richardson JE, Ringwald M, Rubin GM, Sherlock G. Gene ontology: Tool for the unification of biology. The gene ontology consortium. *Nature genetics*. 2000;25:25-29
5. Rodella LF, Rezzani R, Buffoli B, Bonomini F, Tengattini S, Laffranchi L, Paganelli C, Sapelli PL, Bianchi R. Role of mast cells in wound healing process after glass-fiber composite implant in rats. *Journal of cellular and molecular medicine*. 2006;10:946-954
6. Rezzani R, Rodella L, Tartaglia GM, Paganelli C, Sapelli P, Bianchi R. Mast cells and the inflammatory response to different implanted biomaterials. *Archives of histology and cytology*. 2004;67:211-217
7. Carpenter AE, Jones TR, Lamprecht MR, Clarke C, Kang IH, Friman O, Guertin DA, Chang JH, Lindquist RA, Moffat J, Golland P, Sabatini DM. Cellprofiler: Image analysis software for identifying and quantifying cell phenotypes. *Genome biology*. 2006;7:R100
8. Maherali N, Ahfeldt T, Rigamonti A, Utikal J, Cowan C, Hochedlinger K. A high-efficiency system for the generation and study of human induced pluripotent stem cells. *Cell stem cell*. 2008;3:340-345
9. Lian X, Hsiao C, Wilson G, Zhu K, Hazeltine LB, Azarin SM, Raval KK, Zhang J, Kamp TJ, Palecek SP. Robust cardiomyocyte differentiation from human pluripotent stem cells via temporal modulation of canonical wnt signaling. *Proc Natl Acad Sci U S A*. 2012;109:E1848-1857
10. Guyette JP, Fakharzadeh M, Burford EJ, Tao ZW, Pins GD, Rolle MW, Gaudette GR. A novel suture-based method for efficient transplantation of stem cells. *J Biomed Mater Res A*. 2013;101:809-818
11. Kelly DJ, Azeloglu EU, Kochupura PV, Sharma GS, Gaudette GR. Accuracy and reproducibility of a subpixel extended phase correlation method to determine micron level displacements in the heart. *Med Eng Phys*. 2007;29:154-162
12. Foroosh H, Zerubia J. Extension of phase correlation to subpixel registration. *IEEE Transactions on Image Processing*. 2002;11:188-200
13. Gaudette GR, Todaro J, Krukenkamp IB, Chiang FP. Computer aided speckle interferometry: A technique for measuring deformation of the surface of the heart. *Ann Biomed Eng*. 2001;29:775-780
14. Liu L, Gardecki JA, Nadkarni SK, Toussaint JD, Yagi Y, Bouma BE, Tearney GJ. Imaging the subcellular structure of human coronary atherosclerosis using micro-optical coherence tomography. *Nat Med*. 2011;17:1010-1014
15. Ha Usler G, Lindner MW. "Coherence radar" and "spectral radar"-new tools for dermatological diagnosis. *Journal of biomedical optics*. 1998;3:21-31
16. Oliphant TE. Python for scientific computing. *IEEE COMPUTER SOC*. 2007;9:10-20
17. Aivazis KJMaM. Python for scientists and engineers. *IEEE COMPUTER SOC*. 2011;13:9-12
18. Du P, Kibbe WA, Lin SM. Improved peak detection in mass spectrum by incorporating continuous wavelet transform-based pattern matching. *Bioinformatics*. 2006;22:2059-2065
19. De Mey S, Thomas JD, Greenberg NL, Vandervoort PM, Verdonck PR. Assessment of the time constant of relaxation: Insights from simulations and hemodynamic measurements. *Am J Physiol Heart Circ Physiol*. 2001;280:H2936-2943
20. Hunter JD. Matplotlib: A 2d graphics environment. *IEEE COMPUTER SOC*. 2007;9:90-95
21. Badylak SF, Valentin JE, Ravindra AK, McCabe GP, Stewart-Akers AM. Macrophage phenotype as a determinant of biologic scaffold remodeling. *Tissue Eng Part A*. 2008;14:1835-1842

VIDEO FILE LEGENDS

Supplemental Video I
µbead perfusion through the conductance artery and microvasculature within the mid-myocardium of a decellularized human heart, acquired using µ-optical coherence tomography (µOCT).

Supplemental Video II
Spontaneously contracting human iPS-derived cardiomyocytes.

Supplemental Video III
Spontaneously contracting cardiac fiber reseeded with human iPS-derived cardiomyocytes.

Supplemental Video IV
Micro-optical coherence tomography of a spontaneously contracting cardiac fiber reseeded with iPS-derived cardiomyocytes.

Supplemental Video V
Strain delivery to the LV wall of a decellularized porcine heart under mechanical stimulation in our bioreactor.

Supplemental Video VI
Recellularized human heart mounted in our human heart bioreactor under perfusion and mechanical stimulation.

Supplemental Video VII
Visible contractions of a reseeded human heart.